AGU PUBLICATIONS

JGR

Journal of Geophysical Research: Atmospheres

RESEARCH ARTICLE
10.1002/2016JD026301

Key Points:
- Comprehensive validation of aerosol optical depth (AOD) at 550 nm from MAIAC Terra and Aqua according to land cover types over South America
- Accuracy of MAIAC AOD_{550} retrievals varies as function of land cover type, AOD magnitude, and climatological seasons in South America
- MAIAC AOD_{550} retrievals are stable over the MODIS Terra and Aqua mission

Correspondence to:
V. S. Martins,
vitorstmartins@gmail.com

Citation:
Martins, V. S., A. Lyapustin, L. A. S. de Carvalho, C. C. F. Barbosa, and E. M. L. M. Novo (2017), Validation of high-resolution MAIAC aerosol product over South America, *J. Geophys. Res. Atmos.*, *122*, 7537–7559, doi:10.1002/2016JD026301.

Received 28 NOV 2016
Accepted 9 JUL 2017
Accepted article online 11 JUL 2017
Published online 26 JUL 2017

Validation of high-resolution MAIAC aerosol product over South America

V. S. Martins[1], A. Lyapustin[2], L. A. S. de Carvalho[1], C. C. F. Barbosa[1], and E. M. L. M. Novo[3]

[1]Image Processing Division, Brazilian Institute for Space Research, São José dos Campos, Brazil, [2]NASA Goddard Space Flight Center, Greenbelt, Maryland, USA, [3]Remote Sensing Division, Brazilian Institute for Space Research, São José dos Campos, Brazil

Abstract Multiangle Implementation of Atmospheric Correction (MAIAC) is a new Moderate Resolution Imaging Spectroradiometer (MODIS) algorithm that combines time series approach and image processing to derive surface reflectance and atmosphere products, such as aerosol optical depth (AOD) and columnar water vapor (CWV). The quality assessment of MAIAC AOD at 1 km resolution is still lacking across South America. In the present study, critical assessment of MAIAC AOD_{550} was performed using ground-truth data from 19 Aerosol Robotic Network (AERONET) sites over South America. Additionally, we validated the MAIAC CWV retrievals using the same AERONET sites. In general, MAIAC AOD Terra/Aqua retrievals show high agreement with ground-based measurements, with a correlation coefficient (R) close to unity (R_{Terra}:0.956 and R_{Aqua}: 0.949). MAIAC accuracy depends on the surface properties and comparisons revealed high confidence retrievals over cropland, forest, savanna, and grassland covers, where more than 2/3 (~66%) of retrievals are within the expected error (EE = ±(0.05 + 0.05 × AOD)) and R exceeding 0.86. However, AOD retrievals over bright surfaces show lower correlation than those over vegetated areas. Both MAIAC Terra and Aqua retrievals are similarly comparable to AERONET AOD over the MODIS lifetime (small bias offset ~0.006). Additionally, MAIAC CWV presents quantitative information with R ~ 0.97 and more than 70% of retrievals within error (±15%). Nonetheless, the time series validation shows an upward bias trend in CWV Terra retrievals and systematic negative bias for CWV Aqua. These results contribute to a comprehensive evaluation of MAIAC AOD retrievals as a new atmospheric product for future aerosol studies over South America.

1. Introduction

Aerosols are suspended solid and liquid particles in the atmosphere derived from natural and anthropogenic sources. Common natural sources are desert dust, volcanoes, wildfire, sea salt, and biogenic compounds from vegetation, while anthropogenic sources include biomass burning from logging and agricultural areas, fossil fuel combustion, and industrial pollution [*Lenoble et al.*, 2013]. South America has a seasonal variability of aerosol burden in the atmosphere caused by industrial emissions in megacities, dust plumes across Patagonia and Atacama deserts and interannual biomass burning in Cerrado (Brazilian savanna) [*Videla et al.*, 2013] and biogenic aerosol from Amazon rain forest [*Artaxo and Hansson*, 1995]. These particles perform a complex function in climate system [*Intergovernmental Panel on Climate Change*, 2013] and bring large uncertainties on aerosol climate forcing [*Carslaw et al.*, 2013]. Thus, many efforts have been made to understand the aerosol physical, chemical, and optical properties [*Yu et al.*, 2006], as well as aerosol-cloud interaction [*Wang et al.*, 2016] and impacts on hydrologic cycle [*Rosenfeld et al.*, 2014].

The AERONET (Aerosol Robotic Network) program fills the knowledge gap of aerosol optical properties [*Holben et al.*, 1998]. The program has an extensive network of sun photometers at global scale that provides long-term database of solar and sky radiance measurements. Direct sun measurements provide spectral aerosol optical depth (AOD or τ) and Ångström exponent (AE or α) at 340–1020 nm [*Holben et al.*, 2001]. The AOD characterizes aerosol loading in the column of atmosphere, and α gives the spectral dependence of AOD, commonly related to the aerosol particle size [*Eck et al.*, 2010]. Thus, this reliable database allows insight on aerosol optical and microphysical properties. However, the limited number of operational ground stations restricts some large-scale applications, where the spatial variability of aerosol is required. In contrast, satellite remote sensing provides global spatial coverage of aerosol with daily

resolution, therefore being a useful data source to understanding aerosol patterns in the atmosphere [*Kaufman et al*., 2002].

Since the beginning of the 21st century, Earth Observation System (EOS) has provided valuable global data from Moderate Resolution Imaging Spectroradiometer (MODIS), enhancing monitoring, modeling, and forecasting of global climate. In MODIS Atmosphere Collection, the "Dark Target" algorithm was developed to AOD retrieval over the dark surface [*Kaufman et al*., 1997], while the "Deep Blue" algorithm is applied over both dark and bright land surfaces [*Hsu et al*., 2004, 2013]. Historical improvements in MODIS aerosol algorithms reveal the efforts for more accuracy and higher quality in satellite aerosol products [*Remer et al*., 2005; *Levy et al*., 2007, 2013]. Multiangle Implementation of Atmospheric Correction (MAIAC) is a recent MODIS algorithm designed to retrieve surface bidirectional reflectance factor, internal cloud mask, column water vapor (CWV), and AOD over land [*Lyapustin et al*., 2011]. In general, MAIAC applies time series approach to dynamically derive surface spectral ratios between MODIS blue at 0.47 μm and shortwave infrared bands at 2.1 μm used for 1 km AOD retrievals over dark and bright surfaces, with exceptions for bright salt pans and snow areas. The multiangle observations from four or more cloud-free measurements are used to derive spectral surface bidirectional reflectance distribution function (BRDF), knowledge of which helps MAIAC smoke/dust detection and improves the accuracy of atmospheric correction. Particularly, it offers an advantage of prior knowledge of surface properties to overcome empirical assumptions from previous standard algorithms. Furthermore, AOD retrievals at 1 km resolution provides fine-scale variability required for many applications, as smoke plume detection [*Lyapustin et al*., 2012] and air pollution studies [*Kloog et al*., 2015].

In this context, continuous validation efforts are vital to consolidate the confidence in aerosol products and their applications [*Chu*, 2002; *Ichoku et al*., 2002; *Levy et al*., 2010; *Sayer et al*., 2013]. While accuracy of MAIAC surface reflectance was thoroughly evaluated over the Amazon basin [e.g., *Hilker et al*., 2012], a critical assessment of MAIAC AOD over South America is missing. Our objective is to perform an extensive validation of MAIAC AOD retrievals with AERONET measurements at continental scale as a function of land cover types —from the Atacama Desert to the Amazon forest in South America. Additionally, we also evaluate the quality of CWV retrievals using the same AERONET sites. This paper is structured as follows: section 2 provides an overview of the MAIAC and AERONET data, and section 3 describes the validation approach. In section 4, we present a comparison of MAIAC versus AERONET for AOD and CWV retrievals. Finally, section 5 presents the conclusions.

2. Data Description

2.1. AERONET Data

The AERONET (Aerosol Robotic Network) is a global network of automatic radiometers that performs measurements of direct solar and sky radiance in several channels at every 15 min interval [*Holben et al*., 1998]. These measurements are used to compute columnar AOD at interval from 350 to 1020 nm based on Beer-Lambert-Bouguer law with expected uncertainties of ~0.01 to 0.021 [*Eck et al*., 1999]. AERONET data are available in three categories: level 1.0 (unscreened), level 1.5 (cloud screened), and level 2.0 (cloud screened and quality assured). In this study, we selected 19 AERONET sites with at least 1 year of quality assured data (level 2.0) within 2000–2015 (Table 1). These sites are geographically distributed over the continent (Figure 1) and are sensitive to several main aerosol types, such as biomass burning, urban pollution, and dust plumes [*Holben et al*., 2001]. As AERONET does not provide measurements at 550 nm, AERONET level 2.0 data were interpolated to 550 nm using quadratic fits on a log-log scale (equation (1)) [*Eck et al*., 1999]

$$\ln\mathrm{AOD} = \beta_2(\ln\lambda)^2 + \beta_1(\ln\lambda) + \beta_0, \tag{1}$$

where β_2, β_1, and β_0 are coefficients derived from multispectral AOD_λ values typically measured at 380, 440, 500, 675, 870, and 1020 nm, and they can be used to interpolate the AOD measurement to 550 nm by equation (1). The curvature β_2 is a reliable proxy of aerosol particle size, where the negative values represent fine-mode particles (radius $\ll$ 1.0 μm) and the positive values are indicative of the coarse mode (radius $>$ 1.0 μm) [*Schuster et al*., 2006]. Second-order interpolation has a satisfactory agreement with AERONET AOD_λ within ~0.01–0.02 [*Eck et al*., 1999].

Table 1. Over-Land AERONET Sites Used in This Study[a]

AERONET Sites	Latitude	Longitude	Elevation (m)	Period	Available AOD Days
Abraços Hill, Brazil (**1**)	10.76°S	62.35°W	200	1999–2005	1125
Alta floresta, Brazil (**2**)	9.87°S	56.1°W	277	1993–2016	3122
Arica, Chile (**3**)	18.47°S	70.31°W	25	1993–2016	3208
Balbina, Brazil (**4**)	1.91°S	59.48°W	80	1993–2003	558
Belterra, Brazil (**5**)	2.64°S	54.95°W	70	1996–2005	856
Campo Grande-SONDA, Brazil (**6**)	20.43°S	54.59°W	677	2003–2016	1547
Casleo, Argentina (**7**)	31.79°S	69.30°W	2552	2011–2014	1101
Ceilap BA, Argentina (**8**)	34.56°S	58.50°W	10	1995–2016	2637
Ceilap RG, Argentina (**9**)	51.60°S	69.32°W	15	2005–2016	838
Cordoba-CETT, Argentina (**10**)	31.52°S	64.46°W	730	1994–2010	1667
Cuiabá-Miranda, Brazil (**11**)	15.72°S	56.02°W	210	2001–2016	2331
Ji Paraná-SE, Brazil (**12**)	10.93°S	61.85°W	218	2000–2016	995
La Paz, Bolivia (**13**)	16.53°S	68.06°W	3439	2005–2016	1467
Manaus Embrapa, Brazil (**14**)	2.89°S	59.96°W	115	2011–2016	511
Rio Branco, Brazil (**15**)	9.95°S	67.86°W	212	1994–2016	2140
Santa Cruz, Bolivia (**16**)	17.80°S	63.17°W	442	1993–2016	1170
São Martinho Sonda, Brazil (**17**)	29.44°S	53.82°W	489	2003–2016	746
São Paulo, Brazil (**18**)	23.56°S	46.73°W	865	2000–2016	1373
Trelew, Argentina (**19**)	43.24°S	65.31°W	15	2000–2016	1927

[a]The ID number in parentheses is a reference to site location in Figure 1.

2.2. MAIAC

MAIAC products are available for the whole missions (Terra and Aqua) and delivered in Hierarchical Data Format. The suite of atmospheric products includes cloud mask, AOD at 0.47 and 0.55 μm gridded at high resolution (1 km), and column water vapor from MODIS near-infrared (NIR) bands at 0.940 μm. Since the publication of *Lyapustin et al.* [2011], MAIAC algorithm has added capability for smoke (dust) detection [*Lyapustin et al.*, 2012], improved aerosol retrieval over bright deserts, improved cloud and snow mask, added aerosol retrievals and atmospheric correction over inland, coastal, and open ocean water, and has undergone considerable changes for global application. Storing multiday records from MODIS, the algorithm adds the knowledge of time series to decouple surface and aerosol information using the following assumption: aerosol events are extremely variable during the daytime and homogeneous at small areas (~30 km^2), while the land surface is typically stable over a short time scale and heterogeneous spatially. A publication, describing MAIAC Collection 6 algorithm, is under preparation and will be available shortly. This study applies MAIAC AOD_{550} (2000–2015) from MODIS C6 Terra and Aqua data collocated with ground-based measurements in the validation approach. Figure 2 shows an example of true-color image of (a) MODIS Terra and (b) MAIAC AOD retrievals acquired on 8 September 2007 over South America. This figure gives an example of MAIAC aerosol retrievals in clear-sky pixels under partly cloudy and clear conditions during biomass burning season.

3. Validation Approach

The validation is a rather standard approach that requires spatial and temporal collocation between satellite (MAIAC) and ground-truth (AERONET) AOD_{550} measurements for statistical evaluation (Figure 3). In section 3.1, we show the evaluation of spatial and temporal window for coincident observations between satellite and ground-truth AOD measurements. Section 3.2 defines the land cover (LC) types around AERONET sites and LC-stratified validation, and section 3.3 presents the statistical indicators.

3.1. Spatiotemporal Window

Ground-based measurements provide a high sampling rate (~15 min) at the local point, while satellite images have large spatial coverage at a short time interval. Direct comparison using only one pixel value located over ground stations or ground measurements obtained at the exact time of satellite overpass restricts the probability for matchup data, due to cloud cover or time delay between satellite and ground-based measurements. Assuming that aerosol plume is relatively homogeneous within a certain time-space boundary

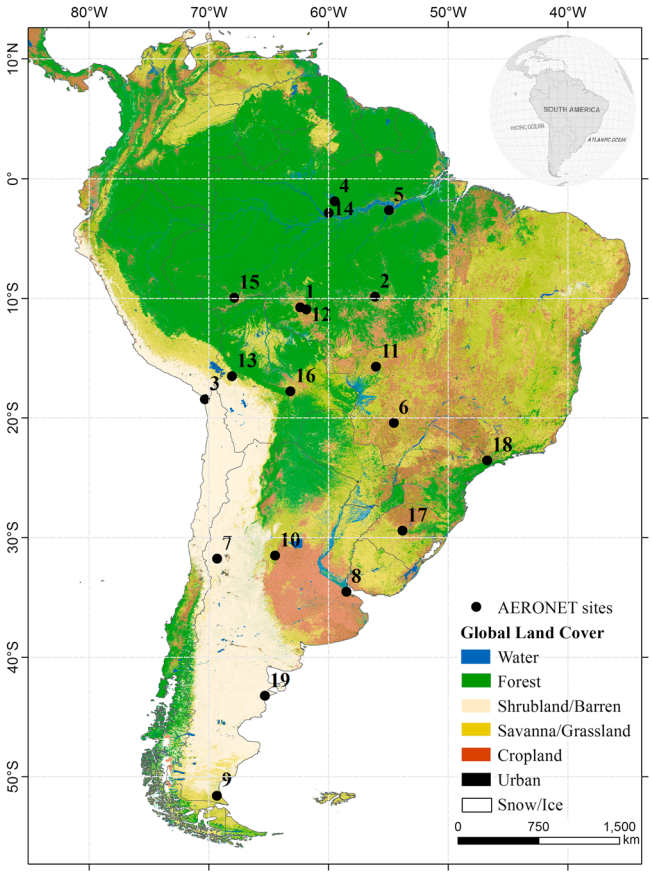

Figure 1. Geographical distribution of the AERONET sites. The ID numbers identify AERONET sites described in Table 1. Background of Global Land Cover product [*Broxton et al.*, 2014] reclassified to seven land cover types.

[*Anderson and Charlson*, 2003], it is pertinent to use the AOD retrievals within some spatial window and time interval has been used for validation [e.g., *Ichoku et al.*, 2002]. For this reason, we perform an average of AERONET measurements for four time intervals (t) from 30 to 120 min centered at satellite overpass to compare it with the average of MAIAC retrievals for five spatial windows (d) from 3 km to 125 km centered at each site point. The selected spatial and temporal window is committed to a better balance between correlation quality and sample size.

Indeed, the highest correlations are expected for the minimum time lag and the smallest window size. From overall statistics for Terra and Aqua products in Table 2, results show little variability in agreement over time lag and window size. The sample size tends to increase with both time and space windows, despite the fact that the case of $d < 75$ km shows fewer matchup pairs than that of $d < 25$ km for MODIS Aqua as result of the average filter that requires at least 40% of valid points. For window of 25 km, the comparisons reveal an increase of matchups and correlations compared to those of the 3 km window for both products, although results remain very close in most cases. Therefore, we selected the 25×25 km^2 as one of the balanced window with reasonable sample size and correlation quality. Additionally, this spatial window is within mesoscale aerosol homogeneity ~50–60 km^2 [*Anderson and Charlson*, 2003], rather similar to 20×20 km^2 used in a previous MAIAC validation [*Lyapustin et al.*, 2011] and close to 25 km radius used for the global validation of MODIS Deep Blue AOD [*Sayer et al.*, 2013].

As observed in Table 2, the time interval has a small impact in the overall agreement for both products, mostly because the average over delta time also includes AOD_{550} values from a previous time threshold. Thus, we selected an interval of ±60 min as a reasonable matchup period, due to sample size increases

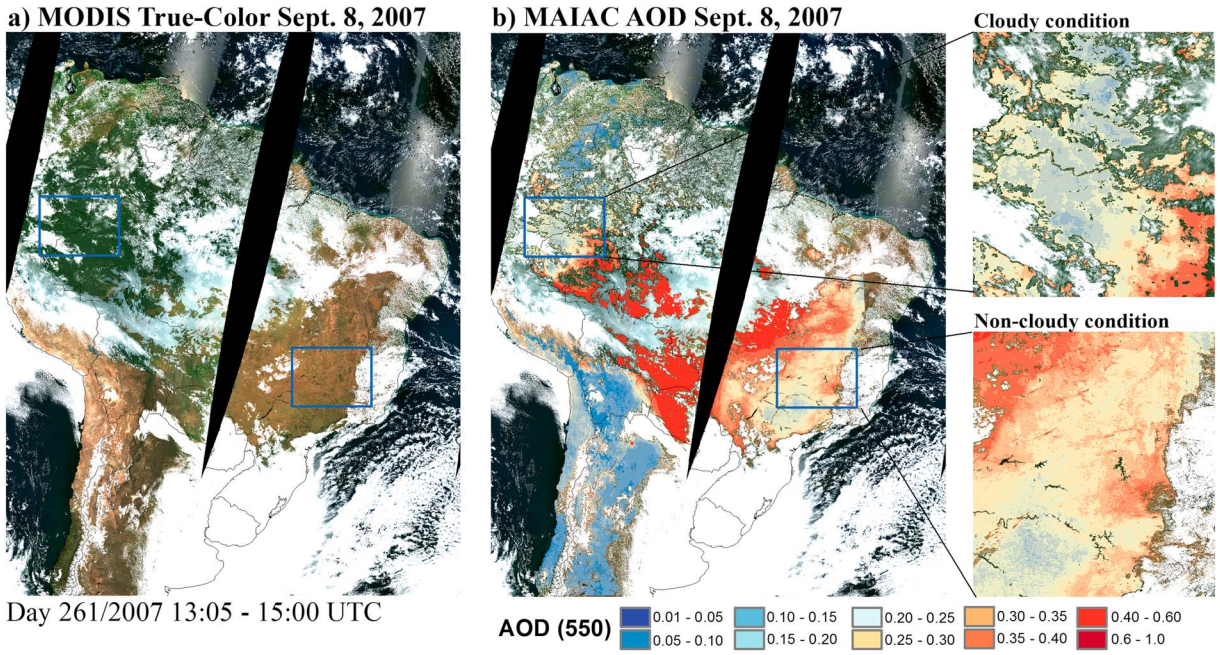

Figure 2. Example of MAIAC aerosol loading on 8 September 2017 (dry season). (a) MODIS true-color image; (b) MAIAC AOD under partly cloudy (top) and clear condition (bottom).

from 8136 (±30 min) to 8575 (±60 min) for Terra using 25 × 25 km^2, and this interval is close to one used for MISR validation [*Kahn et al*., 2005]. Therefore, the validation approach applies the average MAIAC retrievals within 25 × 25 km^2 centered at each site compared to an average of AERONET measurements within ±60 min around the time of the satellite overpass.

3.2. Land Cover Around AERONET Sites

Since satellite algorithms rely on surface spectral properties to decouple atmosphere and surface contributions, the land cover introduces background context to understand the limitations of MAIAC AOD_{550} retrievals. Global Land Cover (GLC) is a MODIS product at 0.5 km spatial resolution that supports our analysis with land cover information around each AERONET site [*Broxton et al*., 2014].

As expected, the global product often presents undesirable classification errors, due to inherent difficulties to distinguish surfaces with similar spectral properties, interannual variability, and limited spatial resolution. In GLC product over Brazil, cropland is often confused with savanna. In particular, cropland areas are significant aerosol sources due to biomass burning and soil particles suspended from tillage practices. For instance, Ji Parana-SE site shows the mean AOD_{550}~ 0.338 with wide variation from 0.018 to 4.76 as influenced by the biomass burning during the winter season [*Hoelzemann et al*., 2009]. Once the importance of these areas

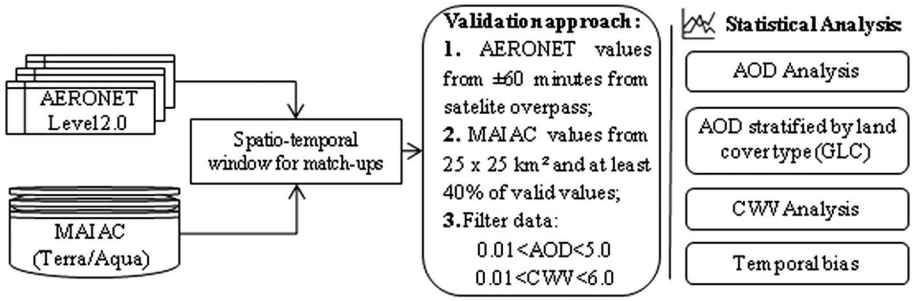

Figure 3. Flowchart of validation approach.

Table 2. Matchup Analysis Applied to Various Spatial (d) and Temporal (t) Window for Terra and Aqua[a]

	$t \leq 30$ min	$\mathbf{t \leq 60}$ **min**	$t \leq 90$ min	$t \leq 120$ min
		TERRA		
$d < 3$ km	7642/0.956	8136/0.952	8372/0.950	8568/0.948
	0.071/−0.016	0.075/−0.015	0.077/−0.015	0.078/−0.015
$d < 15$ km	7916/0.957	8443/0.955	8681/0.953	8877/0.952
	0.069/−0.020	0.072/−0.019	0.074/−0.019	0.078/−0.015
$\mathbf{d < 25}$ **km**	8017/0.958	**8575/0.956**	8813/0.954	9017/0.953
	0.068/−0.024	**0.071/−0.023**	0.072/−0.023	0.074/−0.023
$d < 75$ km	7981/0.953	8615/0.952	8889/0.951	9104/0.950
	0.072/−0.032	0.075/−0.032	0.076/−0.032	0.076/−0.032
$d < 125$ km	8232/0.949	8998/0.946	9376/0.944	9627/0.943
	0.074/−0.030	0.077/−0.031	0.078/−0.032	0.079/−0.032
		AQUA		
	$t \leq 30$ min	$\mathbf{t \leq 60}$ **min**	$t \leq 90$ min	$t \leq 120$ min
$d < 3$ km	6060/0.949	6459/0.945	6653/0.943	6799/0.941
	0.076/−0.005	0.078/−0.006	0.079/−0.006	0.081/−0.006
$d < 15$ km	6341/0.954	6733/0.949	6919/0.947	7076/0.946
	0.071/−0.014	0.075/−0.015	0.076/−0.015	0.077/−0.016
$\mathbf{d < 25}$ **km**	6340/0.954	**6740/0.949**	6931/0.947	7083/0.946
	0.071/−0.019	**0.075/−0.020**	0.075/−0.021	0.076/−0.021
$d < 75$ km	6182/0.948	6602/0.944	6802/0.943	6965/0.942
	0.072/−0.029	0.0741/−0.029	0.074/−0.030	0.074/−0.031
$d < 125$ km	6259/0.942	6716/0.939	6932/0.938	7099/0.938
	0.075 /−0.029	0.077/−0.030	0.077/−0.031	0.077/−0.031

[a]First line: Number of matchups/correlation coefficient, second line: RMSE/bias. The selected time-space threshold is presented in bold.

was recognized, we refined the GLC information over savanna areas using the agricultural areas classified by the Brazilian Institute of Geography and Statistics (IBGE). The IBGE is an official institute that provides the classification of land cover and land use based on MODIS time series, OLI/Landsat-8 and Rapid-Eye images, and field information [*Brazilian Institute of Geography and Statistics*, 2016]. Here the savanna and pasture of GLC product were overlaid by agricultural areas from IBGE classification.

The first level of GLC types was reclassified into seven generic land covers (see Figure 1). From these classes, we extracted the cover types within 25 × 25 km^2 window around each AERONET to group these sites as function of major land cover (at least 50%) (Table 3). The mixed group includes all AERONET sites without a predominant land cover type (less than 50%). Table 3 shows the similarity between AERONET AOD mean and standard deviation stratified by land cover types. Indeed, a quite similar AOD regimes is expected when particles are driven by the same aerosol sources, although boundary conditions, such as elevation, topography, surface features, and wind transport, might change the aerosol distribution and patterns.

The AERONET program clearly concentrates efforts on exploring aerosol dynamic under several environmental conditions [*Holben et al*., 2001]. Table 4 shows land cover distribution around the selected AERONET sites. This distribution reveals aerosol monitoring efforts near land features susceptible to wildfire and biomass burning events, such as savanna, grassland, and cropland, over South America.

Since the aerosol type depends on origin and transport, these particles are directly related to the surface type and its typical sources [*Lenoble et al*., 2013]. Note that although local aerosol sources influence on aerosol regimes, long-range transport can also change the background aerosol in remote areas [*Andreae*, 2007]—for example, Saharan dust and biomass burning smoke transported by trade wind from Africa reach the Amazon basin [*Baars et al*., 2011]. To explore the relation of AOD and Ångström exponent for each land cover type, Figure 4 presents a scatterplot for AOD and the Ångström exponent with distinct patterns among land covers. The coarse-mode particles (median radius > 0.6 μm and $\alpha_{440-670} < 0.5$) observed over barren and sparse vegetation is also common in desert regions [*Basart et al*., 2009]. The fine-mode particles (median radius < 0.6 μm and $\alpha_{440-670} \sim 1.2$–$1.5$) are most frequent for continental sources, as urban pollution with AOD ~ 0.2 to 1.0. For the cropland group, the biomass burning season

Table 3. Basic Statistics of AERONET Sites Grouped According to Major Land Cover Type

Land Cover	AERONET Sites	Major Land Cover (%)	AOD_{550} (mean ± std)
Forest	Balbina	58.95	0.179 ± 0.110
	Manaus Embrapa	76.68	0.192 ± 0.151
Shrubland/Barren	Casleo	100	0.024 ± 0.018
	Trelew	86.78	0.035 ± 0.028
Savanna/Grassland	Ceilap RG	66.34	0.022 ± 0.013
	Cordoba CETT	56.03	0.080 ± 0.065
	Santa Cruz	50.84	0.183 ± 0.173
Cropland	Abraços Hill	62.84	0.338 ± 0.369
	Alta Floresta	64.68	0.253 ± 0.392
	Cuiabá Miranda	71.36	0.233 ± 0.334
	Ji Paraná SE	71.68	0.338 ± 0.494
	Rio Branco	62.89	0.248 ± 0.304
Urban	Ceilap BA	76.78	0.089 ± 0.075
	São Paulo	90.77	0.214 ± 0.150
Mixed	Arica	—	0.219 ± 0.107
	Belterra	—	0.209 ± 0.171
	Campo Grande	—	0.127 ± 0.198
	La Paz	—	0.084 ± 0.045
	São Martinho	—	0.071 ± 0.078

changes the aerosol burden that increases to high AOD values (~1.5–3.5) and small particle size ($\alpha_{440-670}$ ~ 1.5–2.0). Therefore, a validation scheme using land cover groups introduces surface background and aerosol context, wherein the typical AOD range varies according to aerosol sources located in each cover type.

3.3. Statistical Analysis

The quality of satellite aerosol products from MODIS Collections using DT and DB algorithms were well documented and globally validated [*Remer et al.*, 2005; *Levy et al.*, 2010, 2013; *Sayer et al.*, 2013]. The historical application of these products is consequence of rigorous validation and evaluation of uncertainties in retrieval process. For DT algorithm, the expected error (EE) envelope was defined as ± (0.05 + 0.15*AOD) over land, containing 2/3 of retrievals (66% or approximately one standard deviation σ) falling within the EE limits [*Remer et al.*, 2005; *Levy et al.*, 2010]. The EE envelope includes the absolute (0.05) and relative (0.15) uncertainties of AOD retrievals, such as surface properties, sensor calibration, aerosol models, and empirical thresholds [*Levy et al.*, 2010]. Although EE limits are a benchmark to evaluate the standard MODIS aerosol product, the performance level of MAIAC algorithm expects to overcome empirical assumptions due to dynamic spectral regression coefficient (SRC) characterization and knowledge of surface spectral BRDF. Thus, we will evaluate the target accuracy of EE envelope assuming the relative error of 0.05 as consequence of MAIAC advances from MODIS Collection 6 (equation (2)) and fraction of retrievals falling within EE envelope calculated by equation (3):

$$EE = \pm(0.05 + 0.05 \times AOD) \quad (2)$$

Table 4. Land Cover Distribution Around AERONET Sites

Land Cover Type	AERONET Sites (%)
Water bodies	7.80
Forests	9.84
Shrubland/Barren	16.25
Savanna/Grassland	22.96
Croplands	25.91
Urban	17.34

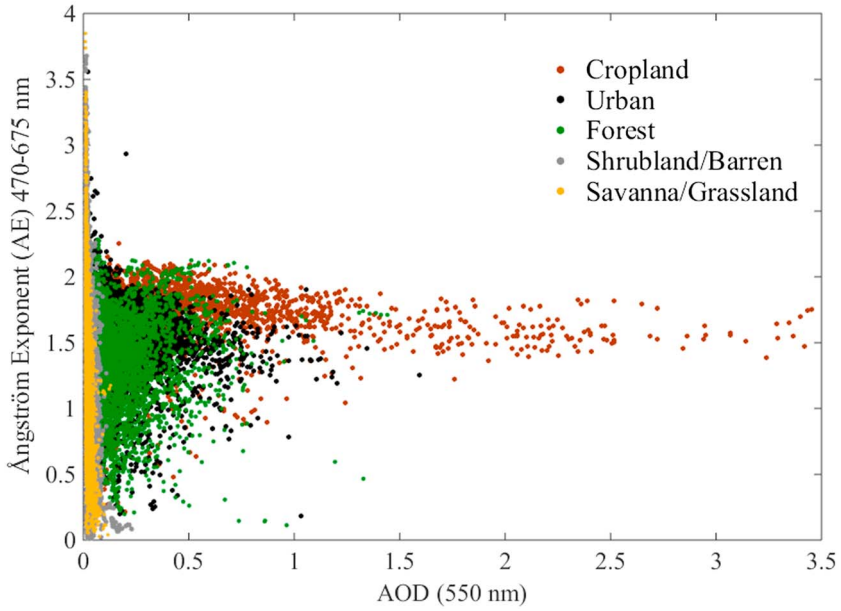

Figure 4. Scatter points of AOD_{550} versus Ångström exponent (440–670 nm) for land cover types. The scatter provides 5000 random pair points from AERONET site per land cover type: Ji-Paraná SE (cropland; brown); São Paulo (urban; black); Manaus Embrapa (forest; green); Casleo (shrubland/barren; gray); and Ceilap RG (savanna/grassland; yellow).

$$AOD - |EE| \leq AOD_{MAIAC} \leq AOD + |EE| \quad (3)$$

Additionally, this validation analysis makes extensive use of the root-mean-square error (RMSE), normalized RMSE (NRMSE), and mean bias (bias) calculated by equations (4)–(6), respectively.

$$RMSE = \sqrt{\left(\frac{1}{n}\sum_{i=1}^{n}(AOD_{MAIAC} - AOD_{AERONET})^2\right)} \quad (4)$$

$$NRMSE = \frac{RMSE}{\overline{AOD}_{AERONET}} \quad (5)$$

$$Bias = \frac{1}{n}\sum_{i=1}^{n} AOD_{MAIAC} - AOD_{AERONET} \quad (6)$$

The $\overline{AOD}$ is the mean value and n is the number of matchups.

4. Results and Discussion

4.1. Overall MAIAC and AERONET AOD_{550} Comparison

Figure 5 shows the scatterplots for MAIAC Terra and Aqua retrievals against simultaneous AERONET measurements. The statistics were fitted with 8575 (Terra) and 6740 (Aqua) matchups from MAIAC products at 19 AERONET sites. The results showed suitable MAIAC retrievals for both Terra and Aqua products, with R close to unity ($R_{Terra/Aqua}$: 0.956/0.949). Both *Remer et al.* [2005] and *Levy et al.* [2010] suggested that aerosol product reaches a satisfactory accuracy when more than 66% of retrievals (2/3 or ~one sigma) falling within EE limits. Using this approach for MAIAC AOD product, our evaluation showed confident retrievals for both MAIAC products with the fraction of retrievals within EE (equation (2)) of 67.9% for Terra and 66.7% for Aqua. For comparison, both MODIS collections 5 (C5) and 6 (C6) had quite similar accuracy to our results, since R is 0.840 for C5 and 0.860 for C6 [*Levy et al.*, 2013]. The quality of MAIAC AOD products is rather similar to the previous MODIS collections but presents substantial advances for retrievals at 1 km resolution and lower relative error in EE (0.15 to 0.05). Our results also show comparable quality retrievals between MODIS

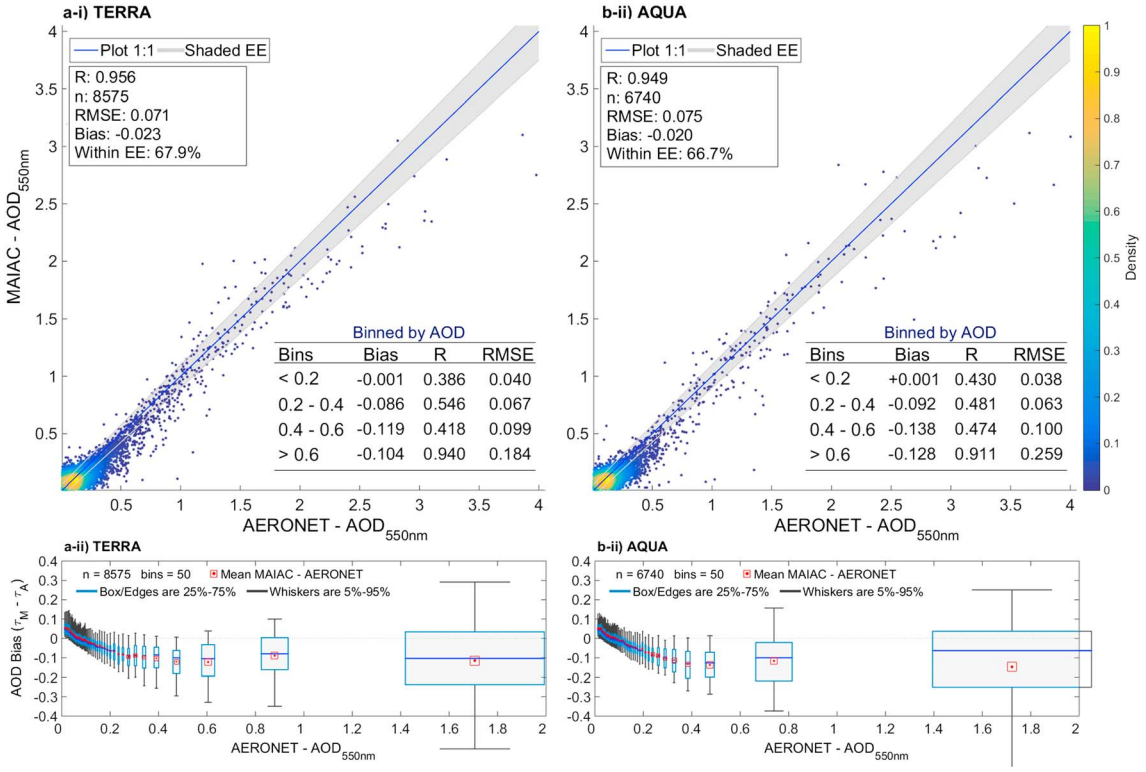

Figure 5. Scatterplots of MAIAC (a) Terra and (b) Aqua against AERONET AOD_{550}. The line 1:1 and MAIAC expected error (EE = ±0.05 ± 0.05 × AOD) are shown in solid blue and shaded gray area, respectively. In top-left text: correlation coefficient (*R*), number of matchups (*n*), and fraction of retrievals within EE. In bottom-right text: statistics binned by AOD intervals.

instruments that allow fine-scale applications using combined Terra and Aqua retrievals. Figures $5a_{ii}$ and $5b_{ii}$ show the bias (*y* axis) versus AOD values (*x* axis) for Terra and Aqua, respectively. The results present distinct bias trend: (i) positive bias up to AOD = 0.1 values and (ii) a low albeit systematic negative bias for AOD values >0.1. At low AOD (<0.1), the surface-related errors lead to a small positive bias, while at high AOD, representing biomass burning, a constrained negative bias indicates the need to refine the regional aerosol model (in particular, by increasing aerosol absorption).

As discussed in section 3.2, the AE acts as a proxy for particle size and bias analysis versus AE is rather instructive to understand aerosol type impacts on AOD retrievals. Figure 6a presents the AOD bias ($\tau_M - \tau_A$) as a function of the AERONET $AE_{470–670\ nm}$ (*x* axis) colored by AERONET AOD retrieved. The matchups were sorted by AE values and then grouped into 50 bins for each statistic box. Figures 6b and 6c represent the bias statistics versus AE values for lower (<0.4) and higher AOD (>0.4), respectively, with box edge of 25–75% and whiskers of 5–95% in each bin. In lower AOD than 0.4 (Figure 6b), MAIAC retrievals have an absolute bias lower than 0.03 regardless of the AE value ($0 < AE < 3.0$). In turn, MAIAC retrievals for AOD higher than 0.4 present a systematic negative bias within AE interval ($0.75 < AE < 2.0$), with negative bias near −0.24 ($AE < 1.6$), and then decrease to –0.15 ($AE > 1.6$). In particular, bias is generally close to 0 (up to ±0.05) for coarse-dominated aerosol ($AE < 0.6$). Similarly, *Superczynski et al.* [2017] reported high AOD bias at coarse or mixed particle sizes ($AE\ 0.5 < AE < 1.75$) with slight negative trend (see Figure 6 therein). Therefore, our main results are slight negative bias trend for low AOD regardless of particle size (to better than 0.03, Figure 6b) and higher negative bias in coarse-dominated conditions (Figure 6c).

Figure 7 shows that the asymmetric distribution of AOD_{550} data set concentrates more than 98% of values between 0.01 and 1.0. The extreme high AOD_{550} (>1.0) represents less than 1.8% of aerosol events that are most driven by agriculture practices, as seen in Figure 3. In general, frequency distribution of both Terra and Aqua products showed significant differences between satellite and ground-based retrievals at low AOD (0.01–0.2), and it decreased exponentially for moderate-high (~0.4–1.0) and extreme high (>1.0) AOD

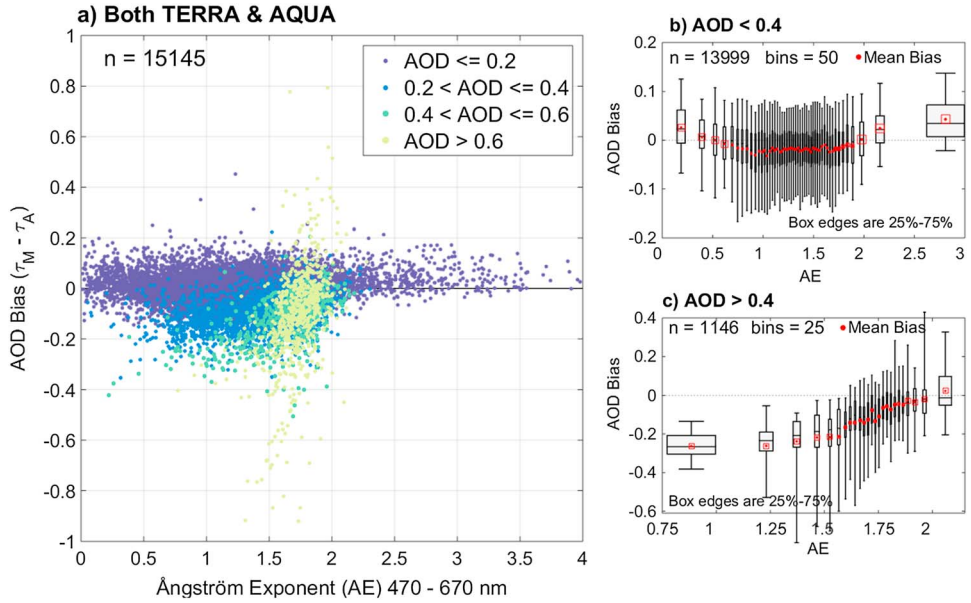

Figure 6. MAIAC-AERONET AOD bias ($\tau_{M\ -}\ \tau_A$) at 550 nm (*y* axis) versus Ångström exponent (AE) from AERONET (*x* axis). (a) AOD bias using all matchups from both Terra and Aqua colored by binned AOD from AERONET retrieval. Matchups are sorted by the AE and grouped into 50 equal bins for (b) lower and (c) higher than 0.4. Each box edge and whiskers represents the 25–75% and 5–95% of data with median (black line) and mean (red point).

values. The highest difference in frequency distribution occurred for low AOD values caused by surface noise on clear atmospheric days. As observed for MOD04 C5, high surface reflectance contributions at low AOD reduce the AOD sensitivity in TOA reflectance [*Levy et al.*, 2010]; however, the absolute error of MAIAC AOD remains small.

4.2. MAIAC and AERONET AOD_{550} Comparison Over Land Cover Types

MAIAC algorithm integrates time series analysis and image processing to decouple surface reflectance and atmosphere properties. Thus, the performance of MAIAC aerosol depends on two key factors: surface type and aerosol properties. The Top-of-Atmosphere (TOA) reflectance is clearly more sensitive to aerosol effects

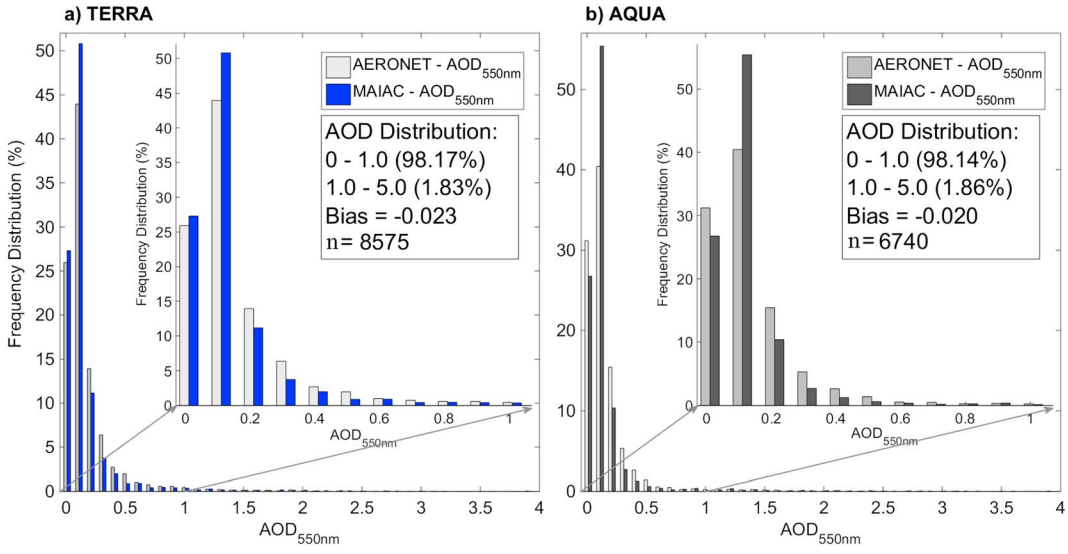

Figure 7. Frequency distribution of MAIAC and AERONET AOD_{550}. Text box: number of AOD_{550} values within interval, bias, and number of matchups (*n*).

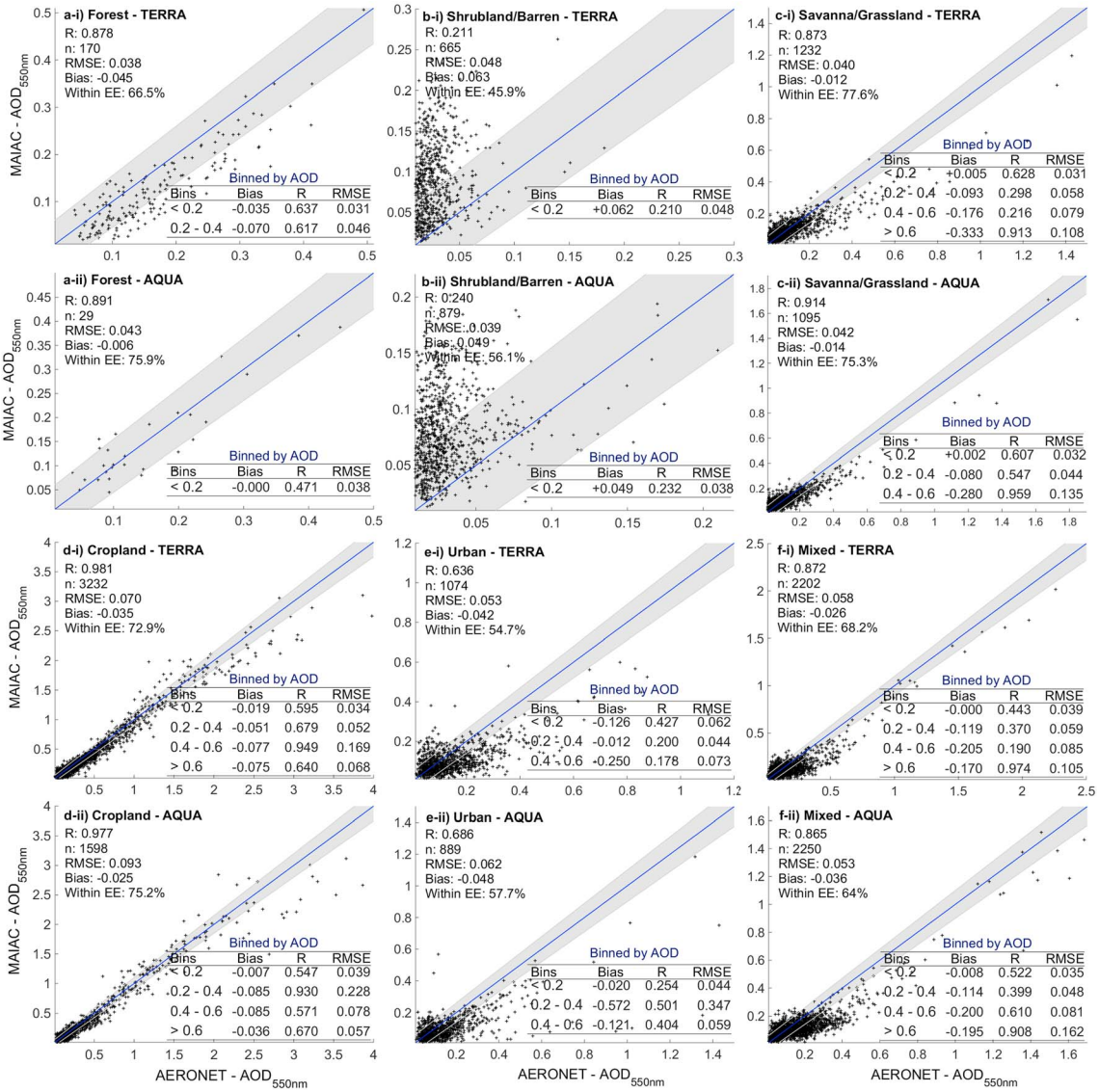

Figure 8. Scatterplots of MAIAC and AERONET AOD_{550} comparisons for land cover types: (a) forest; (b) shrubland and barren; (c) savanna and grassland; (d) cropland; (e) urban; and (f) mixed areas. The MAIAC Terra (i) and Aqua (ii) are presented for each land cover. The line 1:1 and MAIAC expected error (EE = ± (0.05 + 0.05 × AOD)) are shown in solid blue and shaded gray area, respectively. In top-left text: correlation coefficient (*R*), number of matchups (*n*), and fraction within EE. In bottom-right text: statistics binned by AOD intervals. At least 15 matchups were required to analysis binned by AOD.

over dark surfaces than over bright surfaces [*Seidel and Popp*, 2012]. Since the background surface properties are essential to aerosol retrievals, the validation of MAIAC is performed considering the land cover types.

Figure 8 shows the MAIAC and AERONET AOD_{550} comparison for individual land cover types. As described, the major land cover type within 25 × 25 km^2 around AERONET site defines the cover group, while the mixed areas include the sites without representative land cover (Table 3). At least 15 matchups were used to bin AOD analysis in each subplot. The sample size ranges from 170 (forest) to 3232 (cropland) matchups for Terra and from 20 (forest) to 2250 (mixed) for Aqua product. Note that AOD range varies for each land cover analysis, due to distinct aerosol sources for each land use and cover type. Our results showed that the AOD retrievals are sensitive to land cover types, where surface properties and AOD magnitude become a key factor to MAIAC performance. *Benas et al.* [2013] evaluated the aerosol products from MODIS and MERIS/AATSR synergy algorithm considering land cover types and also identified the dependence on surface albedo and aerosol microphysics. In summary, MAIAC retrievals were more accurate and better correlated with AERONET measurements over forest, cropland, mixed, savanna, and grassland than those of urban,

shrubland, and barren areas. For comparison, the highest overall correlation was for retrievals over cropland areas, with R near to unity (R_{Terra} : 0.981 and R_{Aqua} : 0.977), and the lowest correlation over shrubland and barren areas—positive bias (+0.062) and low R (R_{Terra}:0.221 and R_{Aqua}:0.24).

In forest areas (Figure 8a), MAIAC and AERONET AOD_{550} comparison showed a good correlation for both products, where R was close to unity (R_{Terra}:0.878 and R_{Aqua}: 0.891). Comparing the two products, MAIAC Aqua had a better EE (75.9%) than that of Terra (66.5%) over forest areas, although both products presented fair accuracy that exceeded the 66% threshold. This difference of EE might be related to delta in sample size (Δn = 170–29 = 141) or cloud cover contrast between the morning and the afternoon orbits [*Hilker et al*., 2015]. This evergreen surface provides temporal stability and strong SRC retrievals that enhance the confidence of surface BDRF at the blue band and aerosol retrieval, as benefits of dense dark vegetation areas [*Kaufman et al*., 1997]. *Petrenko and Ichoku* [2013] also confirmed the suitability of forest surfaces to AOD retrievals and found correlation coefficient higher than 0.84 for multiple sensors (MODIS, MISR, and POLDER) compared with AERONET measurements. In our case, the dense Amazon rain forest around Manaus-Embrapa and Balbina sites explains the algorithm success, as these dark vegetated surfaces increase the sensibility of aerosol dynamics in TOA reflectance. Nevertheless, moderate scattering might be related to the ensemble of aerosol types and cloud residual. *Artaxo et al.* [2013] showed a high variability of aerosol properties in the Amazon region caused by the mixture of biomass burned and organic fine-mode particles, wherein the single scattering albedo (SSA) changes from 0.84 in the wet season to 0.91 in the dry season. In general, forest areas provide feasible surface condition to accurate AOD retrievals and MAIAC products exhibited acceptable retrievals (to lower than absolute error of 0.05) with biases of −0.045 and −0.006 for Terra and Aqua, respectively.

The shrubland and barren areas are arid climate regions with sparse vegetation coverage (~10–20%) of perennial and drought-resistant plants, gravels, and sandy soil. We found the poorest agreement between MAIAC and AERONET AOD_{550} measurements for these arid areas compared to all other land covers (Figure 8b). For Patagonia and Atacama deserts, the bright surfaces and typical low AOD introduce challenging boundary conditions for satellite aerosol retrievals. As seen in Figure 8b, the high biases ($bias_{Terra}$: 0.063 and $bias_{Aqua}$: 0.049) at low AOD might be explained by SRC underestimation and inherent difficulty to decouple atmosphere-surface signal over bright surfaces. Consequently, satellite AOD may show a high noise and a positive bias over these areas, for instance as observed in one extreme case with MAIAC AOD_{550} of 0.29 compared to AERONET of 0.04. The typical low AOD regimes across Patagonia and Atacama regions, as seen in Trelew (0.082 ± 0.058) and Casleo (0.028 ± 0.018) sites, clearly illustrate the sensitivity limits of MAIAC retrievals over barren and bright land surfaces at high spatial resolution.

Figure 8c shows meaningful MAIAC retrievals over savanna and grassland areas, where scatter of points was closer to the 1:1 line with slight negative bias and R exceeding 0.85 for both sensor products. There is a quite similar fraction of AOD retrievals within EE (Terra: 77.6% and Aqua: 75.3%) and mean bias of −0.012 and −0.014 for Terra and Aqua, respectively. The savanna biome in the central Brazil faces intensive land use change and local fire practices during the dry season [*Chen et al*., 2013].Thus, MAIAC time series benefits aerosol retrievals over these regions with seasonal surface changes. Furthermore, since savanna and grassland surfaces cover more than one-quarter (~28%) of South America, reliability of MAIAC retrieval allows routine monitoring of the smoke plumes.

During the dry season, agriculture and pasture areas are hot spots for natural and human-induced fires over South America, and satellite AOD retrievals have been used in biomass burning monitoring over these areas [*Hoelzemann et al*., 2009]. Figure 8d shows that MAIAC retrievals over cropland areas had a better agreement with AERONET measurements than that of all other cover types, with R close to unity (Terra: 0.981 and Aqua: 0.977) and higher fraction of retrievals within EE (Terra: 72.9% and Aqua: 75.2%) than 66% for both products. In comparison, the overall correlation of MAIAC Terra was slightly better than that of Aqua. *Benas et al.* [2013] also showed good AOD retrievals for MERIS/AATSR synergy algorithm (R: 0.68) and MOD04 C5 (R: 0.81) over cropland areas. These managed areas experience a dramatic surface change throughout the agricultural cycle, with distinct surface conditions during soil preparation, crop planting, and harvest periods. Since MAIAC approach partly relies on stable surface condition, the rapid change of surface properties still represents a certain challenge for unbiased aerosol retrievals over agricultural areas—although our results do not show any systematic issue.

MAIAC and AERONET AOD_{550} comparison over urban areas is shown in Figure 8e. Note that these retrievals had spread scatter points at low AOD values and a slight tendency to underestimate values ($bias_{terra}$: − 0.042 and $bias_{Aqua}$: −0.048). MAIAC performed better over urban areas than over shrubland and barren areas but not as well than over vegetated areas. The fraction of retrievals within EE from Aqua (57.7 %) was better than that of Terra (54.7 %) and quite similar to fraction from shrubland and barren areas (56.1 %). This difference suggests that Aqua product is more appropriate for urban retrievals. In general, urban features impose many challenges for satellite aerosol retrievals at high resolutions, such as (i) multiple anthropogenic sources and a high ensemble of aerosol optical properties and (ii) bright surfaces with a mixture of concrete building and roads. In our study case, the urban retrievals used two AERONET sites located in big cities of South America: Buenos Aires and São Paulo. These complex urban areas produce a high contribution in TOA reflectance that reduces sensitivity of measurements to aerosols. For comparison, MOD04 AOD retrievals historically present an overestimation over bright surfaces due to poor surface characterization [*Oo et al*., 2010]. Furthermore, the multiple pollutant sources also contribute to the ensemble of aerosol microphysics which represents a difficulty for aerosol models used in satellite retrievals. *Castanho et al*. [2008] showed the seasonal variation of SSA_{550} (0.75–0.96) over São Paulo and performed a sensitivity analysis showing that the uncertainties of 0.1 in SSA_{550} lead to at least 20% of error in AOD retrievals. Therefore, the spread scatter of points for urban retrievals might be explained by the discrepancy between the model and the actual aerosol microphysical properties. In contrast with our results, *Lyapustin et al.* [2011] validated MAIAC retrievals with UCLA AERONET site located in Los Angeles/EUA and showed the satisfactory correlation with *R* of 0.873, respectively. This contrast with our results might be related to a large ensemble of urban aerosol types and limitation of a fixed aerosol model in MAIAC.

Mixed areas represent all sites without one major land cover type within 25 × 25 km^2. Figure 8f shows that MAIAC and AERONET measurements agree well over mixed areas, with the *R* exceeded 0.85 and mean bias was close to unity ($bias_{Terra}$: − 0.026 and $bias_{Aqua}$: − 0.036). The fraction of retrievals within EE_{Terra} of 68.2% and within EE_{Aqua} of 64% shows that the algorithm succeeded in obtaining satisfactory retrievals (2/3 or 66%) for MAIAC Terra. To understand if a particular mixture of cover types directly influences AOD retrievals, we performed a correlation analysis for each AERONET site with mixed land cover types, as shown in Table 5. The results showed an agreement between MAIAC and AERONET measurements with *R* higher than 0.612 for all sites. Comparing retrievals between sites, Campo Grande and São Martinho showed higher quality retrievals over a mixture of cropland, savanna, and grassland covers, with *R* exceeding 0.72 and fraction of retrievals higher than of 77% within EE for both sensor products. In particular, Belterra site had insufficient number of matchups due to high cloud cover in the Amazon region, which compromises the consistency of the correlation results. Note that correlation analysis for Arica and La Paz sites showed fair agreement between MAIAC and AERONET AOD_{550}, where the spatial window had more than 30% area covered by shrubland and barren covers. Therefore, AOD retrievals were not directly affected by bright surfaces when the spatial window included other land cover types, especially, dark surfaces. This reasonable accuracy over mixed areas suggests that SRC algorithm is quite efficient for heterogeneous surfaces, even over transition areas, e.g., land and ocean transition over Arica site. Therefore, coastal regions without routine aerosol observations, such as the East Coast of Brazil, benefit with quality MAIAC retrievals.

4.3. Impacts of AOD Magnitude

The satellite aerosol retrieval improves with higher aerosol contribution to TOA reflectance. Hence, AOD magnitude is a key factor in the confidence and quality of the retrievals. Figure 9 shows the assessment of MAIAC retrievals according to AOD intervals using the correlation coefficient and NRMSE. These two metrics are sufficient to express the agreement and relative error, where the best retrievals are close to *R* ~1 and NRMSE ~0. Our analysis used the aerosol regimes broken down into AOD intervals: low (0.01–0.2), moderate (0.2–0.4), moderate-high (0.4–0.6), and high (>0.6) AOD values.

In general, our results pointed out that MAIAC and AERONET AOD_{550} correlation decreases when the AOD values decline for the same land cover. On clear days (AOD < 0.2), we found the critical correlation (<0.3) and high NRMSE (>1.2) over shrubland and barren areas, due to inherent difficulty in decouple surface and aerosol contributions at low AOD. Thus, two reasons emerge from our results: (i) TOA reflectance is less sensitive to aerosol loading over a bright surface, and (ii) satellite retrievals at low AOD values are more susceptible

Table 5. Basic Statistics of MAIAC Retrievals From Terra (First Line) and Aqua (Second Line) Compared to AERONET Measurements From Mixed Group Land Cover (%)

Mixed Group	Sensor	Bias	*R*	Within EE (%)	Water	Forest	Shrubland/Barren	Savanna/Grassland	Cropland	Urban
Arica	TERRA	−0.118	0.708	20.0	44.15	----	47.33	0.68	0.10	7.74
	AQUA	−0.092	0.648	32.7						
Belterra	TERRA	----	----	----	33.85	39.68	----	2.61	23.87	----
	AQUA	----	----	----						
Campo Grande	TERRA	−0.003	0.980	85.7	----	0.45	----	32.81	37.23	29.50
	AQUA	−0.010	0.971	83.2						
La Paz	TERRA	0.001	0.561	83.4	----	----	32.69	42.73	----	24.58
	AQUA	0.008	0.612	86.77						
São Martinho	TERRA	0.021	0.783	77.3	0.29	4.63	0.03	47.27	47.48	0.29
	AQUA	0.012	0.873	86.9						

to background surface noises. *Fraser and Kaufman* [1985] introduced the implications of surface reflectance and aerosol absorption to satellite AOD retrievals. The authors described surface reflectance with no variation in TOA reflectance to AOD changes, as critical surface reflectance (CSR). Based on that aerosol loading has distinct effects in TOA reflectance according to surface reflectance, where the aerosol effects increase TOA reflectance over the dark surface and decrease over the bright surface. In the same way, *Hsu et al.* [2004] demonstrated that the TOA reflectance is not sensitive to AOD changes over bright surfaces due to the predominance of aerosol absorption. Therefore, the land cover areas with surface reflectance close to CSR, as urban and desert areas, imply less or no sensitivity to aerosol effects in TOA reflectance. Moreover, *Seidel and Popp* [2012] also showed significant errors of AOD retrievals when the surface reflectance is close to CSR, when 0.01 uncertainty of surface reflectance introduces at least 0.1 error in AOD retrieval. In our study, the poorest results over urban and desert areas might be associated with inaccuracies of surface characterization, and consequently, background effects in AOD retrievals. Conversely, dark surfaces increase aerosol sensitivity due to lower reflectance than CSR. Thus, both products presented better correlation over vegetated areas than that over bright surfaces at low AOD values, and Terra retrievals showed a slightly better correlation than that of Aqua over forest and cropland areas.

Next, the moderate/moderate-high AOD interval (0.2–0.6) led to higher correlations for all covers compared to low AOD results. The agreement for moderate AOD values benefits MAIAC applications over distinct

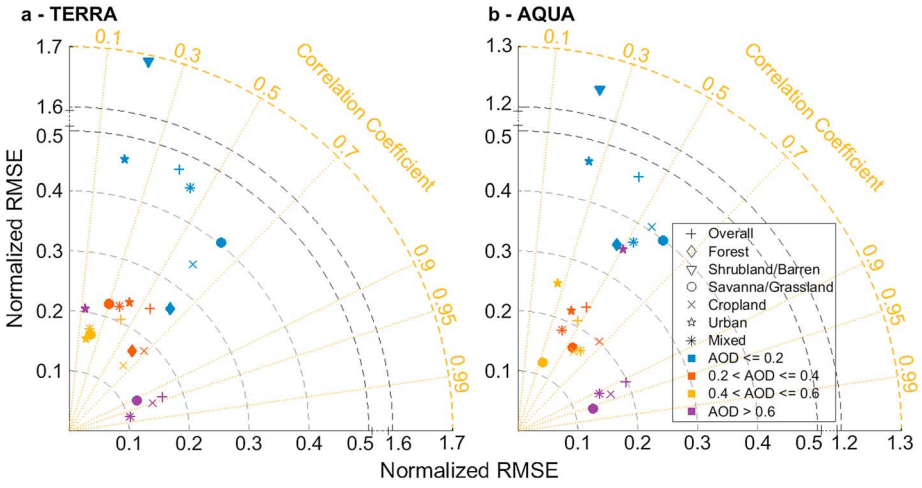

Figure 9. Correlation analysis of AOD intervals using normalized RMSE versus correlation coefficient. Note the discontinuity in NRMSE axis. At least 15 matchups were required to perform this correlation analysis.

regions, since almost all AERONET sites showed average AOD close to 0.2 (Table 3). At high AOD values, correlation analysis showed the clustering of land cover results in low NRMSE (<0.2), and high R (>0.9), with exception for urban retrievals. The multiple scattering regimes of high AOD increase aerosol contribution to TOA reflectance and, consequently, reduce the impacts of surface background. In summary, MAIAC retrievals presented satisfactory correlations for moderate and high AOD (>0.2) over forest, cropland, savanna, and grassland areas. For comparison of Terra and Aqua products, the accuracy of both MAIAC products was quite similar over all AOD range. In applications at low AOD values, a caution should be exercised over bright surfaces, as presented for shrubland and barren areas.

4.4. Impacts of Seasonal Variability on AOD Retrievals

Seasonal analysis of aerosol distribution over South America supports temporal evaluation of MAIAC retrievals. Figure 10 shows the spatial distribution of mean AOD_{550} from $MAIAC_{Terra}$ (2000–2015) for seasonal time scales: DJF (December, January, and February), MAM (March, April, and May), JJA (June, July, and August), and SON (September, October, and November). In general, South America has the aerosol patterns driven by three main continental aerosol types: biomass burning, mineral dust, and urban pollution.

During the austral winter season (SON), the emissions from local fires increase atmospheric turbidity and contribute to strong aerosol seasonality over South America. In the March-April-May season, fire practices are regularly used to open landscapes for agriculture and pasture areas in Colombia, Ecuador, and Venezuela [*Videla et al*., 2013]. The dry season is the critical aerosol period for biomass burning emissions in central-western Brazil. From Abraços Hill and Alta Floresta sites (Table 1), it is observed that seasonal aerosol changes from low AOD during MAM season (0.084 ± 0.05 and 0.076 ± 0.037, respectively) to ~6 times higher in the SON season (0.551 ± 0.414 and 0.571 ± 0.525, respectively). Particularly, September is a dry peak and the most critical month for air quality in central South America, where the maximum AOD reaches 3.1 in the Abraços Hill and 4.72 in the Alta Floresta site. Furthermore, later dry season in northwestern South America delays the onset of the burning season, with drastically change of aerosol loading in DJF season [*Schafer et al*., 2008].

In the desert and arid regions, mineral particles are suspended and transported into the atmosphere due to dust and sand storms, as observed in Atacama and Patagonia deserts [*Ginoux et al*., 2012]. In the first half of the year, Casleo site records typical low AOD_{550} (0.023 ± 0.014) and high mixture of fine and coarse-mode particles ($\alpha_{440-670}$: 1.3 ± 0.9, see Figure 4) during windblown dust in the central region of Patagonia desert. In the DJF period, high amounts of mineral particles are transported from Sahara desert to the Caribbean region and the Northeastern Brazil, which annually changes the atmosphere burden in these regions [*Kaufman et al*., 2005].

Air pollution is a health issue over most populated cities in South America, such as São Paulo, Buenos Aires, and Santiago [*Bell et al*., 2006]. The industrial pollution and fossil fuel combustion influence the local climate and atmospheric turbidity over these cities. In São Paulo site, the smoke plumes increased AOD_{550} by about 1.6 times from the first half of the year (0.167 ± 0.099) to the austral spring (0.268 ± 0.185). Air quality control for these big cities demands routine observation of fine particulate matter emissions that are potentially predicted by satellite AOD products [*Chudnovsky et al*., 2013].

Since sun photometer measurements are the primary benchmark for evaluating satellite aerosol retrievals, an extensive coverage is useful for quality assurance. Figure 8 showed that the Northwestern and Eastern regions still lack the long-term monitoring by AERONET sites, and aerosol microphysical assumptions may be an issue over these regions. Furthermore, the complex topography of the Andes Mountains, located in West South America, represents a challenge surface feature for AOD retrievals and also limits the establishing of continuous aerosol observations. *Shi et al.* [2011] identified high AOD biases between MODIS and MISR products over complex surface features, as the Andes Mountains and the West Coast of the U.S. Although some regions have scarce ground-based observations, the selected AERONET sites are located in regions sensitive to seasonal aerosol records, and validation of MAIAC retrievals using those measurements allowed a critical assessment over different aerosol sources and surface context.

Table 6 presents the statistical indicators (bias, R and fraction within EE) of MAIAC versus AERONET AOD_{550} for quarter seasons (DJF, MAM, JJA, and SON). In general, MAIAC retrievals were sensitive to seasonal aerosol loading over South America, and the overall correlation was higher for the second half of the year (JJA and SON) than that for the first half of the year (Table 6a). In comparison, both sensor products showed a quite

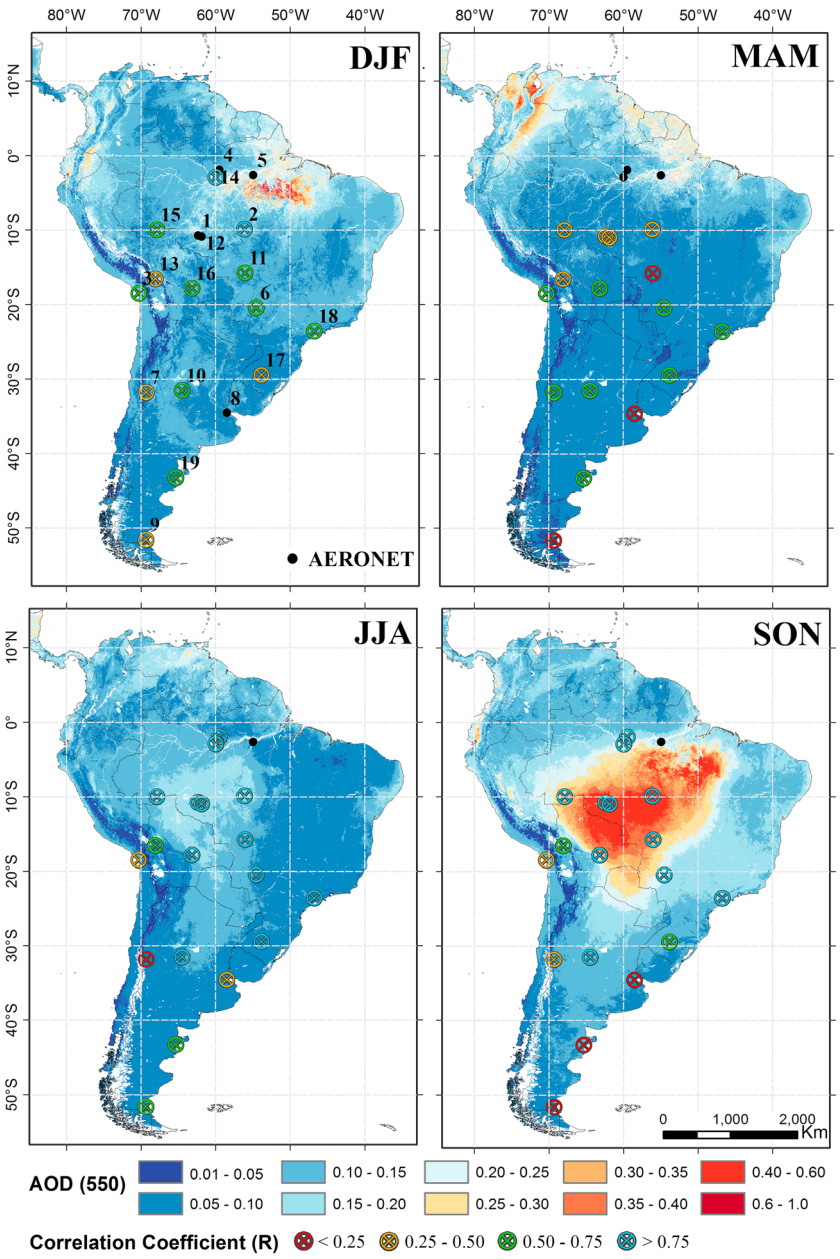

Figure 10. Spatial distribution of average MAIAC AOD_{550} within 2000–2015 for seasonal time scales: DJF (December-January-February), MAM (March-April-May), JJA (June-July-August), and SON (September-October-November). At least 15 matchups of MAIAC versus AERONET measurements were used to compute correlation coefficient per season.

similar correlation throughout the seasons, although it is rather instructive to consider the quality difference between Terra and Aqua products. As discussed by *Hoelzemann et al.* [2009] and observed in Figure 10, the austral winter (SON) is a critical period to burning events and accurate retrievals in the second half of the year enable fine-scale monitoring of smoke plumes over cropland, savanna, and grassland areas (Tables 6d and 6e). So our results show that a good performance of MAIAC retrievals benefit the biomass burning studies related to extreme aerosol regimes over South America, with *R* close to unity for both product (*R* of ~0.975 over cropland); although the fraction of retrievals within EE was lower than 66% in the SON season for both sensors. Similarly, MAIAC retrievals over urban areas showed a relative high *R* (Terra: 0.779 and Aqua: 0.814) during the winter season (Table 6f) and absolute bias lower than 0.1 for all seasons. Furthermore, Aqua retrievals have a higher EE than those of Terra in the urban area, and aerosol applications might consider to use this

Table 6. Temporal Assessment of MAIAC Products for Seasons: DJF (December–February), MAM (March–May), JJA (June–August), and SON (September–November)[a]

Period		Bias	*R*	EE (%)	Bias	*R*	EE (%)	Bias	*R*	EE (%)
		Overall			*Forest*			*Shrubland/Barren*		
DJF	TERRA	−0.010	0.580	62.17	−0.033	0.927	81.25	0.063	0.250	47.03
	AQUA	0.004	0.598	61.39	*n**	*n**	*n**	0.057	0.231	54.76
MAM	TERRA	−0.016	0.528	71.16	*n**	*n**	*n**	0.050	0.248	52.97
	AQUA	−0.008	0.579	72.61	*n**	*n**	*n**	0.040	0.165	67.70
JJA	TERRA	−0.024	0.960	75.2	−0.040	0.913	75.29	0.056	0.035	49.18
	AQUA	−0.029	0.932	70.82	−0.001	0.930	88.23	0.041	0.142	58.02
SON	TERRA	−0.034	0.971	57.39	−0.061	0.799	46.55	0.081	0.096	34.68
	AQUA	−0.028	0.968	58.52	*n**	*n**	*n**	0.059	0.136	41.83
		Savanna/Grassland			*Cropland*			*Urban*		
DJF	TERRA	−0.012	0.688	77.78	0.003	0.715	78.81	−0.016	0.200	58.72
	AQUA	−0.003	0.639	74.24	0.027	0.494	65.00	−0.018	0.117	58.47
MAM	TERRA	−0.001	0.684	87.07	−0.015	0.183	77.67	−0.03	0.539	66.79
	AQUA	−0.006	0.679	82.24	−0.006	0.112	75.86	−0.034	0.299	68.91
JJA	TERRA	−0.006	0.914	75.91	−0.03	0.981	78.52	−0.059	0.572	47.33
	AQUA	−0.015	0.930	76.69	−0.02	0.977	83.04	−0.073	0.694	52.16
SON	TERRA	−0.027	0.882	71.23	−0.065	0.979	56.34	−0.055	0.779	47.52
	AQUA	−0.025	0.932	69.59	−0.055	0.973	57.10	−0.041	0.814	55.90

[a]For each season, first line is of Terra retrievals (shaded gray) and second line is of Aqua retrievals. *n**: insufficient number of matchups ($n < 15$).

sensor product in urban air pollution studies. In shrubland and barren areas, Table 6c shows that correlation parameters also vary seasonally and retrievals during the first half of the year had a better agreement than those of the second half. However, variability of aerosol regime over these areas does not provide an increase in MAIAC accuracy, since Atacama and Patagonia deserts have a typical low AOD patterns throughout the year (Table 3). In particular for forest areas (Table 6b), the high cloud cover on the Amazon rain forest region during the first semester limited the number of matchups and does not guarantee the consistency of the analysis. For the austral winter, MAIAC retrievals showed relative high confidence level over forest areas with *R* close to unity ($R \sim 0.92$). In summary, although overall validation in Figure 5 reported the satisfactory accuracy of AOD retrievals following new expected error (equation (3)), this temporal analysis stratified by land cover type shows that level of algorithm performance also varies with time scale seasons.

4.5. Time Series Validation

As MODIS missions exceed their designed lifetime of 6 years, MODIS Characterization Support Team have been sustaining efforts to monitor the instrument performance and maintain well-calibrated MODIS data throughout the entire mission [*Xiong et al*., 2016]. The calibration issues, spacecraft operation, solar diffuser degradation, and nonfunctional detectors are revised constantly to guarantee the stable calibration and consistence of data records [*Toller et al*., 2013]. Due to calibration updates, Collection 6 MODIS L1B data record promises overcome the long-term calibration artifacts in both MODIS Terra and Aqua [*Xiong et al*., 2016; *Lyapustin et al*., 2014a]. So regarding the concerns with temporal MODIS residual drift in AOD retrievals (e.g., see section 6.3 in *Levy et al.* [2015]), we provide an annual bias analysis to assess the harmonization of two MODIS instruments during mission lifetime. Figure 11 presents the time series validation of Terra and Aqua retrievals within 2002–2015. To reduce the aerosol diurnal variations and surface change properties, we selected only matchups of MAIAC and AERONET measurements acquired on the same day for both sensors (Table 7).

Our results show that AOD bias per year remains quite similar between Terra and Aqua in 15 year period (offset of ~0.006) with minimal temporal dependence in its trend (MAE lower than 0.027). Note that the minimum offset was expected for AOD retrievals from twin MODIS sensors, while AOD biases vary according to

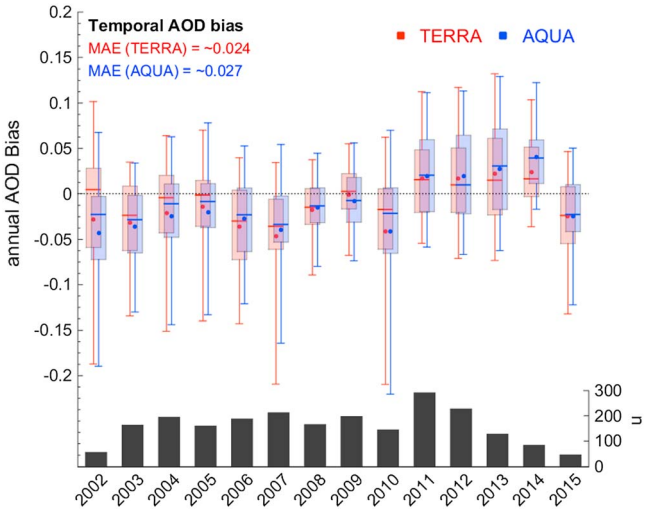

Figure 11. Intercomparison of MAIAC Terra versus Aqua AOD retrievals in time series validation. The sample size (*n*) per year used to bias calculation and MAE is the mean absolute error (MAE).

surface-atmosphere condition in time series. For example, *Aragao et al.* [2014] shows that fire events and their intensity increase during drought years (e.g., El Niño years), such as 2007, 2010, and 2015. On these years of high AOD, MAIAC shows a negative bias, consistently with our analysis above, and no trend. On the regular years, the statistics is dominated by lower AOD and the surface-related contribution with lower cloudiness, where MAIAC shows a positive bias. A small apparent increase in AOD bias during 2011–2014 may be an artifact caused by reduced biomass burning in regular years, both moving MAIAC AOD bias in the positive direction. As a conclusion, this analysis shows a good cross calibration between MODIS Terra and Aqua [*Lyapustin et al.*, 2014a], resulting in consistent AOD products, and general lack of trend over 14 year period. If any residual calibration trend exists, it should not exceed ~0.03 AOD over 14 years. *Sayer et al.* [2013] compared the performance of Deep Blue algorithm between C5 and C6 and also reported improvements in AOD retrievals using C6 calibration.

4.6. Validation of Columnar Water Vapor

Until now, all results in this paper have been focused on MAIAC aerosol retrievals. Additionally, here we present the validation of MAIAC CWV retrievals using the coincident AERONET CWV measurements. The algorithm retrieves column water vapor (cm) using MODIS near-IR bands at 0.94 μm (B17–B19) [*Lyapustin et al.*, 2014b] based on modified version of *Gao and Kaufman* [2003]. This method applies two 2-channel ratios to compute the water vapor transmittance, and then, the amount of water vapor using look-up-table procedures. It is a rather straightforward method that does not assume the linearity of surface reflectance in 0.9–0.94 μm region, contrary to *Gao and Kaufman* [2003]. This technique is susceptive to noise in CWV retrievals when spectral surface properties change in used window region (0.9–0.94 μm), large solar and view geometries or unexpected inconsistence of sensor calibration [*Lyapustin and Wang*, 2008]. While the Algorithm Theoretical Basis Document [*Lyapustin and Wang*, 2008] provided validation of MAIAC CWV for about 150 AERONET sites, this is a first peer-reviewed publication of CWV validation.

In this study, we evaluate the accuracy of MAIAC CWV retrievals using the same spatiotemporal window discussed for AOD in section 3.1: comparison of average MAIAC CWV retrievals within 25 × 25 km^2 with

Table 7. Long-Term AERONET Sites Used in Time Series Validation

AERONET Sites	Latitude	Longitude	Matchups[a]	Period
Alta Floresta, Brazil	9.87°S	56.1°W	448	1993–2016
Campo Grande Sonda, Brazil	20.43°S	54.59°W	491	2003–2016
Casleo, Argentina	31.79°S	69.30°W	548	2011–2014
Ceilap BA, Argentina	34.56°S	58.50°W	600	1995–2016
Cordoba CETT, Argentina	31.52°S	64.46°W	752	1994–2010
Cuiaba Miranda, Brazil	15.72°S	56.02°W	763	2001–2016
Rio Branco, Brazil	9.95°S	67.86°W	201	1994–2016
São Paulo	23.56°S	46.73°W	399	2000–2016

[a]Only matchups from the same day for both MODIS sensors.

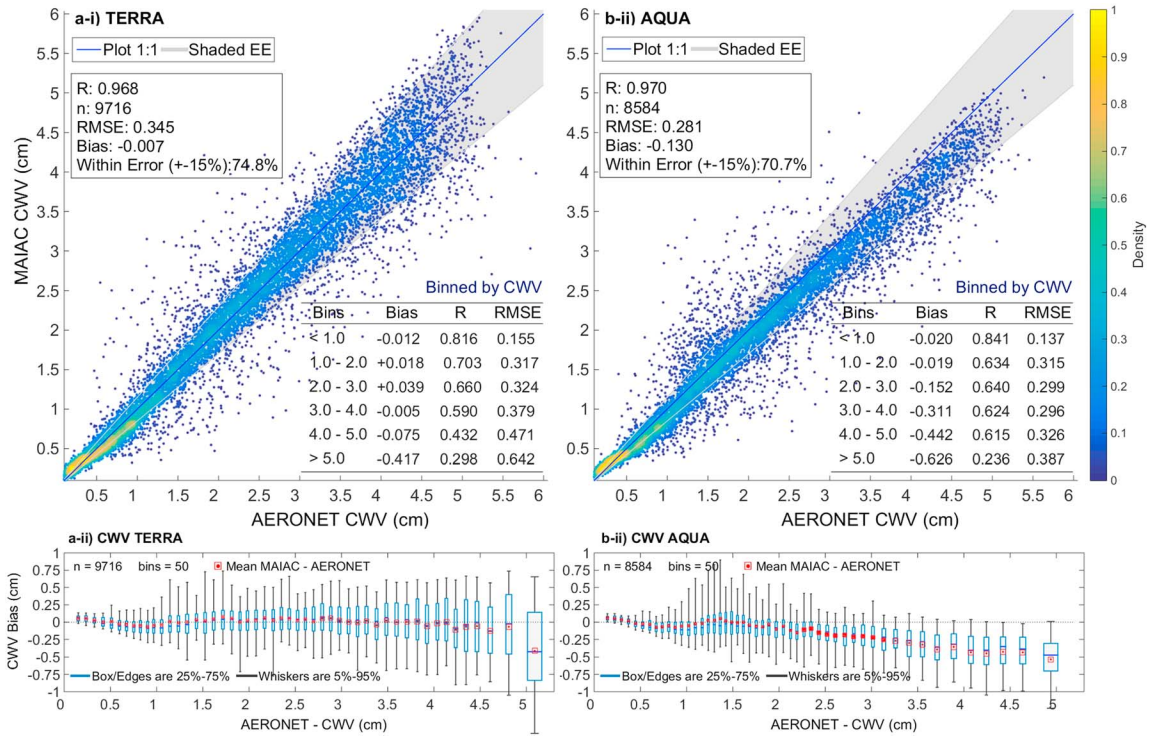

Figure 12. Scatterplots of MAIAC (a) Terra and (b) Aqua against AERONET measurements of columnar water vapor (CWV). The line 1:1 and MAIAC CWV error (±15%) are shown in solid blue and shaded gray area, respectively. In top-left text: correlation coefficient (*R*), number of matchups (*n*), and fraction of retrievals falling within error of ±15%. In bottom-right text: statistics binned by CWV intervals.

AERONET CWV measurements within ±60 min of satellite overpass. The matchup data were filtered between 0.1 and 6.0 cm. The validation of CWV retrievals is shown in Figure 12 with sample number of 9716 and 8584 for MAIAC Terra and Aqua, respectively. Both MAIAC Terra and Aqua provide quantitative information, with more than 70% of retrievals falling within error of ±15% (74.8% and 70.7% for Terra and Aqua, respectively). The results show a fair correlation with the AERONET data (R_{Terra}: 0.968 and R_{Aqua}:0.97), and analysis binned by CWV presents a higher correlation in lower bins (CWV $<$ 1.0 cm with R_{Terra} of 0.816). A 10% systematic negative bias is observed for Aqua retrievals for CWV $>$ 2.0 cm (Figure 12b_{ii}), while Terra shows none trend regardless the concentration (Figure 12a_{ii}). Given the different sensitivity of NIR channels [*Gao and Kaufman*, 2003], the algorithm computes the average of water vapor based on weighting functions stored in the look-up table, which depends on atmosphere condition ("dry" or "humid") (see more details in *Lyapustin et al.* [2014b]). Thus, described negative bias should be related to calibration of the least absorbing channel (B17) of MODIS Aqua which has the highest weight in humid conditions. To understand if MAIAC CWV retrievals are temporally stable and consistent for both MODIS instruments, we also provide a time series validation using matchups averaged annually (Figure 13).

Our results in Figure 13 revealed an offset between Terra and Aqua retrievals during sensor mission. They show previously observed negative bias of MODIS Aqua CWV. Importantly, they also show a consistent systematic upward trend in Terra CWV throughout the mission. MODIS Aqua shows a smaller upward trend up until 2008, when the drifting stopped. Although recent studies of MODIS radiometric performance did not report any calibration issues for MODIS near-IR channels (B17–19) (see Table 1 in *Toller et al.* [2013] and Figures 7 and 8 in *Angal et al.* [2015]), these results suggest an instrument calibration drift or sensor degradation during mission lifetime. Several studies have evaluated the impact of sensor degradation in visible and near-infrared bands [*Lyapustin et al.*, 2014a], AOD retrievals [*Levy et al.*, 2010], and vegetation index [*Wang et al.*, 2012], and our results draw attention to artificial temporal trends in CWV retrievals as well as in standard MODIS CWV product MOD05. This result shows the need for the calibration trend study in MODIS bands 17–19, which were not a part of MODIS Collection 5–6 calibration analysis.

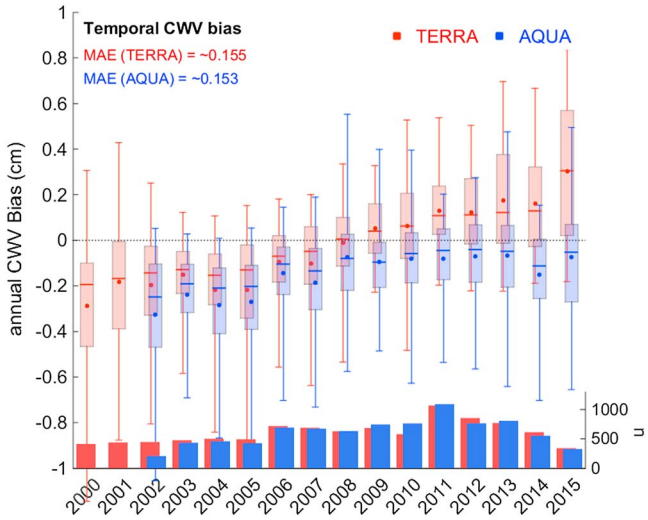

Figure 13. Time series analysis of annually averaged CWV bias of MAIAC Terra versus Aqua CWV retrievals. The CWV bias and sample size (*n*) per year of MAIAC Terra and Aqua are in red and blue, respectively. MAE is the mean absolute error.

5. Conclusion

In the present study, we compared the AOD_{550} retrievals from MAIAC and 19 AERONET sites over South America within a 15 year period (2000–2015). The validation data set includes a typical interval of AOD between 0.01 and 4.0, with average of 0.177. This data set presented AOD records from multiple aerosol sources, such as biomass burning, desert dust, and urban pollution. The MAIAC AOD product from Terra and Aqua presented similar quality retrieval, and the overall comparison with ground-based measurements showed a good correlation for both products, with bias up to −0.023 and *R* close to unity (~0.95). For comparison, these results slightly improve on MOD04 Collection 6 data set; however, the lower relative error in EE envelope (EE = ±(0.05*AOD +0.05)) and high 1 km resolution represent an advantage to fine-scale applications compared to MOD04 resolution (DT-land at 3 and 10 km [*Remer et al*., 2013]).

Algorithm performance was analyzed as a function of the land cover type. MAIAC retrievals showed better agreements with AERONET measurements over forest, savanna, grassland, cropland, and mixed areas, with fraction of AOD retrieval within EE varying from 64 to 77.6%, and *R* exceeding 0.86 for both products. In contrast, MAIAC retrievals over bright surfaces were poorer than those over vegetated areas, with fraction within EE varying from 45.9 to 57.7% and *R* between 0.21 and 0.686. Indeed, these results are expected due to inherent difficulty to decouple surface-atmosphere signals at high surface reflectance and low AOD regimes. Additional correlation analysis over mixed areas showed a satisfactory accuracy for MAIAC retrievals (*R*: 0.561–0.980), even with bright surface contributions around the sites (e.g., Arica and La Paz sites). Thus, our results suggest that MAIAC algorithm performed well over heterogeneous surfaces and the mixture of cover types attenuates the impact of bright surface contributions. Besides land cover types, AOD magnitude influences on quality of MAIAC retrievals. Our analysis showed better confidence for AOD higher than 0.2 values, while the low AOD (<0.2) requires an operational filter to remove some high AOD values, particularly, over bright surfaces. Seasonal aerosol distribution defines distinctive periods over South America and reasonable MAIAC retrievals in the second half of the year benefit several aerosol applications during critical biomass burning season.

In the time series validation, the low offset (~0.006) between Terra and Aqua retrievals shows a temporal stability of MAIAC C6 products. If there is any residual trend from calibration (after major MODIS C6 trends were removed), it is not expected to exceed approximately 0.03 error in 14 years. In general, our main results showed that MAIAC AOD retrievals are useful with good confidence over dark surfaces ($R > 0.86$ and within EE > 66%), especially, for AOD higher than 0.2. Additionally, MAIAC CWV validation shows that more than over 72% of retrievals falling within error of 15% with $R \sim 0.97$. However, a 10% systematic negative bias in MAIAC Aqua at CWV > 2 cm, and upward trend in MAIAC Terra and Aqua prior to 2008 indicate an

instrument calibration drift or sensor degradation during the mission lifetime. We suggest further evaluation of radiometric quality of B17–19 channels for future CWV retrievals.

Finally, MAIAC algorithm offers a new perspective for consistent AOD retrieval at 1 km resolution using explicit surface characterization in terms of spectral BRDF and spectral reflectance ratios. A prior information of surface properties from MODIS time series promises overcomes constraints imposed by empirical assumptions used by standard aerosol algorithms. A comprehensive validation of new multiangle MODIS product supports aerosol studies over South America, and we recommend an extensive MAIAC validation over other regions in the world.

Acknowledgments

We would like to acknowledge the NASA and MODIS team for the maintenance of satellite aerosol products. The work of V.S. Martins was funded by the Coordination for the Improvement of Higher Education Personnel (CAPES) Program. We thank Y. Wang for updating MAIAC data available at ftp://dataportal.nccs.nasa.gov/DataRelease/SouthAmerica/. We also thank AERONET PIs (B. Holben, P. Artaxo, E. Pereira, and E. Quel) for providing sun photometer data. Global Land cover product is available at http://landcover.usgs.gov/global_climatology.php and IBGE land cover at ftp://geoftp.ibge.gov.br/informacoes_ambientais/. We also thank Andrew Sayer and the anonymous reviewer for their helpful comments.

References

Anderson, T., and R. Charlson (2003), Mesoscale variations of tropospheric aerosols*, *J. Atmos. Sci.*, *60*, 119–136.

Andreae, M. O. (2007), Aerosols before pollution, *Science*, *315*, 50–51, doi:10.1126/science.1136529.

Angal, A., X. Xiong, J. Sun, and X. Geng (2015), On-orbit noise characterization of MODIS reflective solar bands, *J. Appl. Remote Sens.*, *9*(1) 094092-094092.

Aragao, L. E., B. Poulter, J. B. Barlow, L. O. Anderson, Y. Malhi, S. Saatchi, O. L. Phillips, and E. Gloor (2014), Environmental change and the carbon balance of Amazonian forests, *Biol. Rev.*, *89*(4), 913–931.

Artaxo, P., and H. C. Hansson (1995), Size distribution of biogenic aerosol particles from the amazon basin, *Atmos. Environ.*, *29*(3), 393–402, doi:10.1016/1352-2310(94)00178-N.

Artaxo, P., et al. (2013), Atmospheric aerosols in Amazonia and land use change: From natural biogenic to biomass burning conditions, *Faraday Discuss.*, *165*, 203, doi:10.1039/c3fd00052d.

Baars, H., A. Ansmann, D. Althausen, R. Engelmann, P. Artaxo, T. Pauliquevis, and R. Souza (2011), Further evidence for significant smoke transport from Africa to Amazonia, *Geophys. Res. Lett.*, *38*, L20802, doi:10.1029/2011GL049200.

Basart, S., C. Pérez, E. Cuevas, J. M. Baldasano, and G. P. Gobbi (2009), Aerosol characterization in Northern Africa, Northeastern Atlantic, Mediterranean Basin and Middle East from direct-sun AERONET observations, *Atmos. Chem. Phys.*, *9*(21), 8265–8282, doi:10.5194/acp-9-8265-2009.

Bell, M. L., D. L. Davis, N. Gouveia, V. H. Borja-Aburto, and L. A. Cifuentes (2006), The avoidable health effects of air pollution in three Latin American cities: Santiago, São Paulo, and Mexico City, *Environ. Res.*, *100*(3), 431–440, doi:10.1016/j.envres.2005.08.002.

Benas, N., N. Chrysoulakis, and G. Giannakopoulou (2013), Validation of MERIS/AATSR synergy algorithm for aerosol retrieval against globally distributed AERONET observations and comparison with MODIS aerosol product, *Atmos. Res.*, *132–133*, 102–113, doi:10.1016/j.atmosres.2013.05.011.

Brazilian Institute of Geography and Statistics (2016), Mudanças na Cobertura e Uso da Terra 2000 – 2010 – 2012 – 2014, 29 pp., Rio de Janeiro. [Available at ftp://geoftp.ibge.gov.br/informacoes_ambientais/cobertura_e_uso_da_terra/mudancas/documentos/.]

Broxton, P. D., X. Zeng, D. Sulla-Menashe, and P. A. Troch (2014), A global land cover climatology using MODIS data, *J. Appl. Meteorol. Climatol.*, *53*(6), 1593–1605, doi:10.1175/JAMC-D-13-0270.1.

Carslaw, K. S., et al. (2013), Large contribution of natural aerosols to uncertainty in indirect forcing, *Nature*, *503*(7474), 67–71, doi:10.1038/nature12674.

Castanho, A. D., J. Vanderlei Martins, and P. Artaxo (2008), MODIS aerosol optical depth retrievals with high spatial resolution over an urban area using the critical reflectance, *J. Geophys. Res.*, *113*, D02201, doi:10.1029/2007JD008751.

Chen, Y., D. C. Morton, Y. Jin, G. J. Collatz, P. S. Kasibhatla, G. R. van der Werf, R. S. DeFries, and J. T. Randerson (2013), Long-term trends and interannual variability of forest, savanna and agricultural fires in South America, *Carbon Manage.*, *4*(6), 617–638, doi:10.4155/cmt.13.61.

Chu, D. A. (2002), Validation of MODIS aerosol optical depth retrieval over land, *Geophys. Res. Lett.*, *29*(12), 8007, doi:10.1029/2001GL013205.

Chudnovsky, A., C. Tang, A. Lyapustin, Y. Wang, J. Schwartz, and P. Koutrakis (2013), A critical assessment of high-resolution aerosol optical depth retrievals for fine particulate matter predictions, *Atmos. Chem. Phys.*, *13*(21), 10,907–10,917, doi:10.5194/acp-13-10907-2013.

Eck, T. F., et al. (2010), Climatological aspects of the optical properties of fine/coarse mode aerosol mixtures, *J. Geophys. Res.*, *115*, D19205, doi:10.1029/2010JD014002.

Eck, T. F., B. N. Holben, J. S. Reid, O. Dubovik, A. Smirnov, N. T. O'Neill, I. Slutsker, and S. Kinne (1999), Wavelength dependence of the optical depth of biomass burning, urban, and desert dust aerosols, *J. Geophys. Res.*, *104*(1), 31,333–31,349, doi:10.1029/1999JD900923.

Fraser, R. S., and Y. J. Kaufman (1985), The relative importance of aerosol scattering and absorption in remote sensing, *IEEE Trans. Geosci. Remote Sens.*, *GE-23*(5), doi:10.1109/TGRS.1985.289380.

Gao, B. C., and Y. J. Kaufman (2003), Water vapor retrievals using Moderate Resolution Imaging Spectroradiometer (MODIS) near-infrared channels, *J. Geophys. Res.*, *108*(D13), 4389, doi:10.1029/2002JD003023.

Ginoux, P., J. M. Prospero, T. E. Gill, N. C. Hsu, and M. Zhao (2012), Global-scale attribution of anthropogenic and natural dust sources and their emission rates based on MODIS deep blue aerosol products, *Rev. Geophys.*, *50*, RG3005, doi:10.1029/2012RG000388.

Hilker, T., A. I. Lyapustin, C. J. Tucker, P. J. Sellers, F. G. Hall, and Y. Wang (2012), Remote sensing of tropical ecosystems: Atmospheric correction and cloud masking matter, *Remote Sens. Environ.*, *127*, 370–384, doi:10.1016/j.rse.2012.08.035.

Hilker, T., A. I. Lyapustin, F. G. Hall, R. Myneni, Y. Knyazikhin, Y. Wang, C. J. Tucker, and P. J. Sellers (2015), On the measurability of change in Amazon vegetation from MODIS, *Remote Sens. Environ.*, *166*, 233–242, doi:10.1016/j.rse.2015.05.020.

Hoelzemann, J. J., K. M. Longo, R. M. Fonseca, N. M. E. Do Rosário, H. Eibern, S. R. Freitas, and C. Pires (2009), Regional representative of AERONET observation sites during the biomass burning season in South America determined by correlation studies with MODIS aerosol optical depth, *J. Geophys. Res.*, *114*, D13301, doi:10.1029/2008JD010369.

Holben, B. N., et al. (1998), AERONET—A federated instrument network and data archive for aerosol characterization, *Remote Sens. Environ.*, *66*(1), 1–16, doi:10.1016/S0034-4257(98)00031-5.

Holben, B. N., et al. (2001), An emerging ground-based aerosol climatology: Aerosol optical depth from AERONET, *J. Geophys. Res.*, *106*(D11), 12,067–12,097, doi:10.1029/2001JD900014.

Hsu, N. C., S.-C. Tsay, M. D. King, and J. R. Herman (2004), Aerosol properties over bright-reflecting source regions, *IEEE Trans. Geosci. Remote Sens.*, *42*(3), 557–569, doi:10.1109/TGRS.2004.824067.

Hsu, N. C., M. J. Jeong, C. Bettenhausen, A. M. Sayer, R. Hansell, C. S. Seftor, J. Huang, and S.-C. Tsay (2013), Enhanced deep blue aerosol retrieval algorithm: The second generation, *J. Geophys. Res. Atmos.*, *118*, 9296–9315, doi:10.1002/jgrd.50712.

Ichoku, C., D. A. Chu, S. Mattoo, Y. J. Kaufman, L. A. Remer, D. Tanre, I. Slutsker, and B. N. Holben (2002), A spatio-temporal approach for global validation and analysis of MODIS aerosol products, *Geophys. Res. Lett.*, *29*(12), 8006, doi:10.1029/2001GL013206.

Intergovernmental Panel on Climate Change (2013), *Climate Change 2013: The Physical Science Basis, Contribution of Working Group I to the Fifth Assessment Report of the Intergovernmental Panel on Climate Change*, edited by T. F. Stocker, et al., pp. 571–675, Cambridge Univ. Press, Cambridge, U. K., and New York, doi:10.1017/CBO9781107415324.

Kahn, R. A., B. J. Gaitley, J. V. Martonchik, D. J. Diner, K. A. Crean, and B. Holben (2005), Multiangle Imaging Spectroradiometer (MISR) global aerosol optical depth validation based on 2 years of coincident Aerosol Robotic Network (AERONET) observations, *J. Geophys. Res.*, *110*, D10S04, doi:10.1029/2004JD004706.

Kaufman, Y. J., A. E. Wald, L. A. Remer, B. C. Gao, R. R. Li, and L. Flynn (1997), The MODIS 2.1-μm channel-correlation with visible reflectance for use in remote sensing of aerosol, *IEEE Trans. Geosci. Remote Sens.*, *35*(5), 1286–1298, doi:10.1109/36.628795.

Kaufman, Y. J., D. Tanré, and O. Boucher (2002), A satellite view of aerosols in the climate system, *Nature*, *419*(6903), 215–223, doi:10.1038/nature01091.

Kaufman, Y. J., I. Koren, L. A. Remer, D. Tanré, P. Ginoux, and S. Fan (2005), Dust transport and deposition observed from the Terra-Moderate Resolution Imaging Spectroradiometer (MODIS) spacecraft over the Atlantic Ocean, *J. Geophys. Res.*, *110*, D10S12, doi:10.1029/2003JD004436.

Kloog, I., M. Sorek-Hamer, A. Lyapustin, B. Coull, Y. Wang, A. C. Just, J. Schwartz, and D. M. Broday (2015), Estimating daily PM2.5 and PM10 across the complex geo-climate region of Israel using MAIAC satellite-based AOD data, *Atmos. Environ.*, *122*, 409–416, doi:10.1016/j.atmosenv.2015.10.004.

Lenoble, J., L. Remer, and D. Tanré (2013), *Aerosol Remote Sensing*, chap. 1, pp. 1–11, Springer, New York.

Levy, R. C., L. A. Remer, S. Mattoo, E. F. Vermote, and Y. J. Kaufman (2007), Second-generation operational algorithm: Retrieval of aerosol properties over land from inversion of Moderate Resolution Imaging Spectroradiometer spectral reflectance, *J. Geophys. Res.*, *112*, D13211, doi:10.1029/2006JD007811.

Levy, R. C., L. A. Remer, R. G. Kleidman, S. Mattoo, C. Ichoku, R. Kahn, and T. F. Eck (2010), Global evaluation of the Collection 5 MODIS dark-target aerosol products over land, *Atmos. Chem. Phys.*, *10*(21), 10,399–10,420, doi:10.5194/acp-10-10399-2010.

Levy, R. C., S. Mattoo, L. A. Munchak, L. A. Remer, A. M. Sayer, F. Patadia, and N. C. Hsu (2013), The Collection 6 MODIS aerosol products over land and ocean, *Atmos. Meas. Tech.*, *6*(11), 2989–3034, doi:10.5194/amt-6-2989-2013.

Levy, R. C., L. A. Munchak, S. Mattoo, F. Patadia, L. A. Remer, and R. E. Holz (2015), Towards a long-term global aerosol optical depth record: Applying a consistent aerosol retrieval algorithm to MODIS and VIIRS-observed reflectance, *Atmos. Meas. Tech.*, *8*(10), 4083.

Lyapustin, A., and Y. Wang (2008), MAIAC-multi-angle implementation of atmospheric correction for MODIS. 77 pp.,Algorithm Theoretical Basis Document (ATBD), NASA.

Lyapustin, A., Y. Wang, I. Laszlo, R. Kahn, S. Korkin, L. Remer, R. Levy, and J. S. Reid (2011), Multiangle implementation of atmospheric correction (MAIAC): 2. Aerosol algorithm, *J. Geophys. Res.*, *116*, D03211, doi:10.1029/2010JD014986.

Lyapustin, A., S. Korkin, Y. Wang, B. Quayle, and I. Laszlo (2012), Discrimination of biomass burning smoke and clouds in MAIAC algorithm, *Atmos. Chem. Phys.*, *12*(20), 9679–9686, doi:10.5194/acp-12-9679-2012.

Lyapustin, A., et al. (2014a), Scientific impact of MODIS C5 calibration degradation and C6+ improvements, *Atmos. Meas. Tech.*, *7*, 4353–4365.

Lyapustin, A., M. J. Alexander, L. Ott, A. Molod, B. Holben, J. Susskind, and Y. Wang (2014b), Observation of mountain lee waves with MODIS NIR column water vapor, *Geophys. Res. Lett.*, *41*, 710–716, doi:10.1002/2013GL058770.

Oo, M. M., M. Jerg, E. Hernandez, A. Picon, B. M. Gross, F. Moshary, and S. A. Ahmed (2010), Improved MODIS aerosol retrieval using modified VIS/SWIR surface albedo ratio over urban scenes, *IEEE Trans. Geosci. Remote Sens.*, *48*(3), 983–1000, doi:10.1109/TGRS.2009.2028333.

Petrenko, M., and C. Ichoku (2013), Coherent uncertainty analysis of aerosol measurements from multiple satellite sensors, *Atmos. Chem. Phys.*, *13*(14), 6777–6805, doi:10.5194/acp-13-6777-2013.

Remer, L. A., et al. (2005), The MODIS aerosol algorithm, products, and validation, *J. Atmos. Sci.*, *62*(4), 947–973, doi:10.1175/JAS3385.1.

Remer, L. A., S. Mattoo, R. C. Levy, and L. A. Munchak (2013), MODIS 3 km aerosol product: Algorithm and global perspective, *Atmos. Meas. Tech.*, *6*(7), 69–112.

Rosenfeld, D., S. Sherwood, R. Wood, and L. Donner (2014), Climate effects of aerosol-cloud interactions, *Science*, *343*(6169), 379–380, doi:10.1126/science.1247490.

Sayer, A. M., N. C. Hsu, C. Bettenhausen, and M. J. Jeong (2013), Validation and uncertainty estimates for MODIS Collection 6 "deep blue" aerosol data, *J. Geophys. Res. Atmos.*, *118*, 7864–7872, doi:10.1002/jgrd.50600.

Schafer, J. S., T. F. Eck, B. N. Holben, P. Artaxo, and A. F. Duarte (2008), Characterization of the optical properties of atmospheric aerosols in Amazônia from long-term AERONET monitoring (1993–1995 and 1999–2006), *J. Geophys. Res.*, *113*, D04204, doi:10.1029/2007JD009319.

Schuster, G. L., O. Dubovik, and B. N. Holben (2006), Ångstrom exponent and bimodal aerosol size distributions, *J. Geophys. Res.*, *111*, D07207, doi:10.1029/2005JD006328.

Seidel, F. C., and C. Popp (2012), Critical surface albedo and its implications to aerosol remote sensing, *Atmos. Meas. Tech.*, *5*(7), 1653–1665, doi:10.5194/amt-5-1653-2012.

Shi, Y., J. Zhang, J. S. Reid, E. J. Hyer, T. F. Eck, B. N. Holben, and R. A. Kahn (2011), Where do we need additional in situ aerosol and sun photometer data?: A critical examination of spatial biases between MODIS and MISR aerosol products, *Atmos. Meas. Tech. Discuss.*, *4*(4), 4295–4323, doi:10.5194/amtd-4-4295-2011.

Superczynski, S. D., S. Kondragunta, and A. I. Lyapustin (2017), Evaluation of the multi-angle implementation of atmospheric correction (MAIAC) aerosol algorithm through intercomparison with VIIRS aerosol products and AERONET, *J. Geophys. Res. Atmos.*, *122*, 3005–3022, doi:10.1002/2016JD025720.

Toller, G., X. Xiong, J. Sun, B. N. Wenny, X. Geng, J. Kuyper, A. Angal, H. Chen, S. Madhavan, and A. Wu (2013), Terra and Aqua moderate-resolution imaging spectroradiometer collection 6 level 1B algorithm, *J. Appl. Remote Sens.*, *7*(1) 073557-073557.

Videla, F. C., F. Barnaba, F. Angelini, P. Cremades, and G. P. Gobbi (2013), The relative role of amazonian and non-amazonian fires in building up the aerosol optical depth in south america: A five year study (2005–2009), *Atmos. Res.*, *122*, 298–309, doi:10.1016/j.atmosres.2012.10.026.

Wang, D., D. Morton, J. Masek, A. Wu, J. Nagol, X. Xiong, R. Levy, E. Vermote, and R. Wolfe (2012), Impact of sensor degradation on the MODIS NDVI time series, *Remote Sens. Environ.*, *119*, 55–61.

Wang, J., et al. (2016), Amazon boundary layer aerosol concentration sustained by vertical transport during rainfall, *Nature*, 1–17, doi:10.1038/nature19819.

Xiong, X., A. Angal, A. Wu, D. Link, X. Geng, W. Barnes, and V. Salomonson (2016), Sixteen years of Terra MODIS on-orbit operation, calibration, and performance, *Proc. SPIE 10000, Sensors, Systems, and Next-Generation Satellites*, *XX*, doi:10.1117/12.2241352.

Yu, H., et al. (2006), A review of measurement-based assessments of the aerosol direct radiative effect and forcing, *Atmos. Chem. Phys.*, *6*, 613–666, doi:10.5194/acp-6-613-2006.